CHALMERS
UNIVERSITY OF TECHNOLOGY

Combustion of waste-derived fuels in Aluminum smelting plants

An investigation for STENA Metall's Aluminum recycling plant

Master's thesis in Sustainable energy systems

PASCAL SCHERZ

Department of Energy and Environment
Chalmers University of Technology
Gothenburg, Sweden 2016

MASTER'S THESIS 2016

Combustion of waste-derived fuels in Aluminum smelting plants

An investigation for STENA Metall's Aluminum recycling plant

PASCAL SCHERZ

CHALMERS
UNIVERSITY OF TECHNOLOGY

Department of Energy and Environment
Division of Energy Technology
CHALMERS UNIVERSITY OF TECHNOLOGY
Gothenburg, Sweden 2016

Combustion of waste-derived fuels in Aluminum smelting plants
An investigation for STENA Metall's Aluminum recycling plant
PASCAL SCHERZ

Supervisor: Thomas Ekvall, Energy and Environment
Examiner: Klas Andersson, Energy and Environment

Master's Thesis 2016:
Department of Energy and Environment
Division of Energy Technology
Chalmers University of Technology
SE-412 96 Gothenburg
Telephone +46 31 772 1000

Cover: A view on the aluminum recycling plant of the STENA METALL AB, which is located in Älmhult, Sweden [STENA METALL AB].

Typeset in LaTeX
Printed by Reproservice (Chalmers printing services)
Gothenburg, Sweden 2016

Combustion of waste-derived fuels
An investigation for STENA Metall's Aluminum recycling plant
PASCAL SCHERZ
Department of Energy and Environment
Chalmers University of Technology

Abstract

Today's industrialized nations produce a steadily rising amount of waste containing huge amounts of valuable plastics and metals (i.e. WEEE, SLF) as well as waste resulting from refinery processes (i.e. PFO). These modern waste streams demand for alternative treatment methods to either expand their usage with recycling or to recover their energy, when recycling is not possible or economically feasible. Especially, intense metallurgic industries are highly dependent on fossil fuels and could benefit with respect to both CO_2 emissions and fuel costs when a co-combustion together with waste-derived fuels would be applied. However, high shares of chlorine, sulfur and other problematic substances present in these modern waste streams can led to environmental and technical difficulties. Before experimental studies need to be done, combustion simulations can help selecting a potential fuel for co-combustion. In this work, seven different waste-derived fuels with differing yearly availabilities, compositions and heating values were investigated, regarding a potential co-combustion with propane in an aluminum recycling process. For the investigation, CHEMKIN PRO simulations were performed for each waste-derived fuel to consider their quantitative effect on the combustion. The results of the simulations together with other evaluation criteria, i.e. several environmental constraints regarding emission limitations and economical boundaries, were used to find the most promising waste-derived fuel for a potential future co-combustion in an aluminum smelting plant. According to the results of this thesis, PFO seems to be the most promising waste-derived fuel to be used in a future co-combustion process.

Keywords: aluminum, co-combustion, emissions, propane, recycling, simulations, waste-derived fuel

Acknowledgements

An economically and environmentally acceptable way of handling upcoming waste sources in terms of energy recovery was one of the driving forces leading this work. The interest to accomplish this project arose, as the regarded field of research is quite unexplored and was expected to lead to a beneficial gain of knowledge, which can support a future research in this area. A special thanks for the successful execution of the project should be acknowledged to the company STENA Metall AB. In particular, I would like to mention Marianne Gyllenhammar, Jilvero Henrik and Björn Hall who have contributed with their readiness and rapid implementation of requests for the successful execution of this project. Furthermore, I would like to thank especially my supervisor Thomas Ekvall as well as my examiner Klas Andersson for their technical, structural and general project-related assistance. Last but not least, I would like to thank my family which has also contributed to the success of this work on a personal level.

Pascal Scherz, Gothenburg, June 2016

Contents

List of Tables

List of Figures

Abbreviations

Abbreviation	Explanation
GHG	Green house gas
PCDD	Polychlorinated dibenzodioxins
PCDF	Polychlorinated dibenzofurans
PFO	Processed fuel oil
PFR	Plug flow reactor
PUR	Polyurethane
URTF	Universal Rotary Tilting Furnace
WEEE	Waste Electric and Electronic Equipment

1. Introduction

The introduction of the Hall-Heroult electrolytic aluminum recovery process initiated commercial primary aluminum production from the ore in the end of the 19th century. Soon after its global commercial production it was noticed that the primary production of aluminum had a high energy demand and was cost intensive. For this reason, an energy saving potential by recycling aluminum arose within the early 20th century [1, 2]. Since then, aluminum manufacturers have steadily optimized their recycling processes, in order to minimize the energy demand and to diminish primary aluminum production. Nowadays, not only an energy reduction from up to 95% for recycled aluminum, also known as secondary aluminum, has been achieved compared to the production of primary aluminum [3, 4], but also the environmental impact has been attenuated. Thereby, harmful red mud, which is a by-product of primary aluminum production, is avoided.
The amount of recycled aluminum has historically been fluctuating as a result of global demand and supply variations depending on political and economical situations. Both world wars led to a temporary increase of recycled aluminum because the consumption of primary aluminum was rising faster than its production could expand [5, 6, 7]. Although the consumption and waste production of aluminum in the EU and the US had a sufficient quantity to generate a technically and economically strong recycling industry with a steady growth, other factors were influencing or inhibiting the market [3]. I.e., technological development in the power supply sector affected an intermediate decrease of the production and consumption of recycled aluminum in the US, where the construction of enormous hydro power damps in the 1960th decreased cost of electricity and made primary aluminum production cheaper, which led to its industrial growth. At that time, secondary aluminum production reached its minimum and was thereby below the level of the 1910th [8]. Within the late 1970th US governmental interest of minimizing discarded aluminum scrap rose and enforced recycling initiatives through regulations and laws. Primarily, political efforts were based on collecting beverage cans and packaging materials in addition to construction material and other waste sources that were partially recycled before. Not only these new regulations but also the steadily increasing efficiency of aluminum recycling processes attracted countries in the EU and caused, soon after the US initiatives, an increase of aluminum collection and recycling [6]. For other nations like Japan, this shift to aluminum recycling instead of its primary production was rather forced than a politically voluntary decision due to the global oil crises, which influenced in an increasing manner the energy prices in the 1980th [3]. Today, the former outstanding position of the US in aluminum recycling is inherited from the EU with 220 recycling facilities and a total throughput of 10.7 Mtons recycled aluminum in 2014, which corresponds to a recycling rate of 77% (excluding exported aluminum scrap) [4].
Considering an environmental point of view, global leading nations are beginning to realize that steadily rising GHG emissions will cause tremendous future problems due to global warming. Therefore, more and more focus has been laid on sustainable ways of using global resources and reserves. Thus, environmental restrictions as well as social

responsibility will force industries to adapt to this new situation by reducing the use of fossil fuels. This could be done either by switching the fuel source completely or partly to a less carbon intense or to a renewable fuel. One option is to use fuels derived from rapidly growing waste sources such as waste electrical and electronic equipment (WEEE) or shredded light fractions (SLF), which are potential future options due to high energy densities and rising availability. Most co-firing fuels of today are biomass based. Thus, research has to be done in order to achieve the knowledge required to utilize these new waste-derived fuels in a proper way [9, 10].
In literature, a few different co-combustion experiments with WEEE a.o. at BSEF (Japan) and Boliden (Sweden) have shown good results with regard to an environmentally safe and economically acceptable handling of flame retardants containing bromine, which is known as an element forming corrosion promoting species during combustion [13]. Thus, it is necessary to investigate potential usability of such fuel regarding co-firing possibilities and its potential effect on emissions. This work will investigate the possibility to use different waste fractions as a fuel. Focus will be on co-combustion with propane in a rotary kiln used for aluminum recycling. The facility is owned by Stena Aluminium located in Älmhult, Sweden. The waste streams included in the work are collected from Stena Recycling International. The aim of this work is to evaluate the waste-derived fuels, with respect to combustion behavior and emissions. The investigation is carried out using the modeling software CHEMKIN PRO.

2. State of the art burner systems

The technological diversity of burner systems is as large as its industrial applicability, therefore extensive consultancy is needed when choosing a burner systems for a special industrial process. This chapter is going to provide a brief overview over existing burner technologies with focus on burner systems related to aluminum recycling processes. It should be mentioned that the naming of burner technologies varies a lot in literature, and is thereby hard to generalize. In this report, the distinction of different burner technologies is based on the "Industrial burner handbook" by Charles E. Baukal.
Some burner systems are more commonly used in other industrial fields than aluminum recycling processes. One example of such system are *thermal radiation burners*, which are generally designed for low temperature applications such as drying [27]. Another system is the *thermal tube burner systems*, which consists of one or more radiant tube, containing the combustion process. Thus, heat is transferred through the walls of the tubes where it is radiated into the load of the furnace as well as distributed by convection [28]. *Radiant wall burners* were historically used for ethylene-cracking and hydrogen-reformation [15, 29]. In the petrochemical industry it is common to use the *natural draft burners* mainly due to its ability to handle the large variation of fuels that are characteristic for these industries [15]. It should be mentioned again that the burner systems named in this section are not used for aluminum recycling processes and are therefore only considered shortly, as the focus of this report investigates burner systems for aluminum recycling processes.

2.1. Fuel mixing

Generally, one can distinguish between two burner design types differing from the mixing point of air and fuel. In nozzle-mixing types, air and fuel are directly mixed and ignited in the nozzle, whereas in pre-mixing types the mixing takes place before ignition (both principles shown in 2.1. Both technologies can be fed with either liquid or gaseous fuels. When liquid fuels are used, ignition is enhanced by air atomization to promote a fine oil droplet formation [15, 16]. However, liquid fuel firing in pre-mixing burners requires more complex fuel feeding technologies, as the incoming liquid has to be finely dispersed and mixed with air before ignition. Additionally, it can be mentioned that pre-mixing burners fired with liquid fuels are often limited in size and efficiency compared to liquid fuel fired nozzle mixing types.

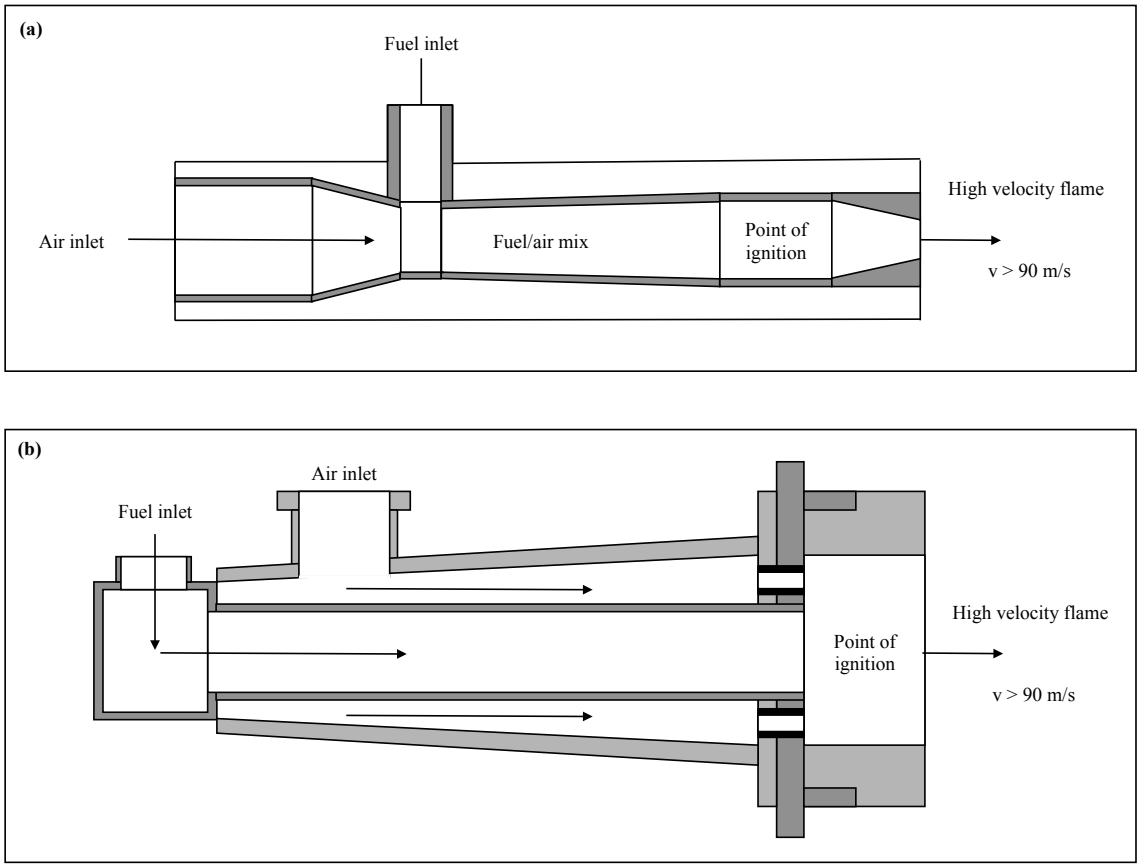

Figure 2.1.: Two schematic pictures showing the difference between (a) pre- and (b) nozzle mixing burners, exemplified for a high-velocity burner

2.2. Staging burners

The oxidizer staging principle, shown in figure 2.2, has the benefit of a better control of the flame shape and length which becomes more uniform compared to premixing burner technologies [20]. This design principle can be easily adapted to most burner types and the ratio of primary and secondary oxidizer can be adapted to match the demand of a specific process. The staging of the oxidizer creates a fuel rich region directly around the point of ignition where usually soot is produced, which leads to a luminous flame and a higher heat flux. In the flame region further from the center, more oxidizer is introduced afterwards, which creates an oxygen rich environment. This principle, therefore, allows a better manipulation of the flame direction, which enhances radiative and convective heat transfer towards the load of the combustion chamber [15]. With the staging principle, NO_x emissions can be lowered, as less oxygen for NO_x formation is available in the high temperature region where its formation is favored and therefore, has several advantages regarding NO_x emission limitations [15].

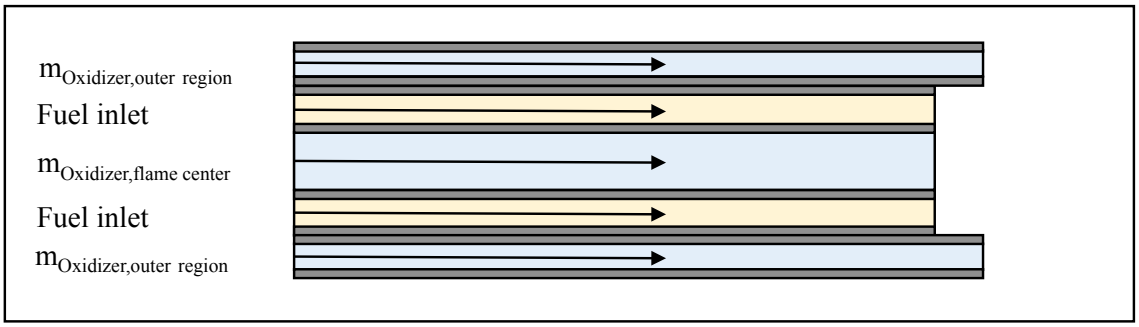

Figure 2.2.: Working principle of oxidizer staging

2.3. Oxidizer lancing

Another option to manipulate combustion conditions and chemistry is to use a secondary oxidizer introduction through a lance. This design is similar to oxidizer staging, explained in the previous section, but differs regarding the injection point of the secondary oxygen. When oxygen lancing is applied, the fuel rich region is extended up to a longer distance from the point of ignition before secondary oxygen is introduced through a lance which can be controlled in position. The simple applicability (also for retrofitting) together with good flame control possibilities and higher temperatures make this principle interesting for aluminum recycling processes [21].
Some potential risks regarding the equipment can occur by using O_2 lancing in certain industrial processes, as the absence of nitrogen and its dilution effect leads to much higher concentration of other corrosion promoting species as i.e. HCl and SO_2. Retrofit designs of existing air/fuel burners using an O_2 lancing system, may potentially lead to higher NO_x emissions (thermal NO_x formation) due to higher flame temperatures, caused by a higher oxygen availability [15, 22].

2.4. High velocity burners

In *high velocity burner systems* the outlet gases usually reach velocities over 90 m/s. This high gas velocity results in a high momentum causing a higher recirculation rate of combustion products and a more uniform temperature profile. All together, this increases the combustion efficiency and can lead to a reduction in fuel consumption compared to burner systems with lower velocities.
Today's state of the art high-velocity burner systems can be designed in several different ways depending on what the process requirements demand for. A mentionable progress featured in most burner systems regards the shape and uniformity of the tile section. This tile section has the purpose of isolating and protecting the internals of the burner and providing a surface where the burner can be mounted. Today, thin and uniformed ceramic tile sections are used, since they offer a better thermal shock resistance compared to previously built thick walled tile sections[15, 16]. It should also be mentioned that some burner designs additionally swirl the inlet air by using guided plates to promote the recirculation zone and with it the combustion [17]. This air swirling concept is not unique for high velocity burners but can also be applied for other burners.

From an aluminum recycling point of view, the benefits with a high velocity burner are given by the temperature uniformity in the furnace as well as the high gas momentum, which promotes heat transfer into tightly packed packages of scrap aluminum. This advantages increase the process performance by a lower residence time for smelting and thus an increasing throughput which results in an increasing aluminum production. Nevertheless, often highly complex designs are applied for such burner concepts, which leads to increased development costs [15, 16].

2.5. Oxygen enriched air burners

One possibility to manipulate combustion temperature and chemistry is to increase the oxygen concentration. In such a combustion system additional oxygen is added to achieve oxygen concentrations over 21%. This is referred to as oxygen enriched air burners, but does not vary a lot in terms of technological design from air/fuel burners (an example is shown in figure 2.3). The Cleanfire HRTM burner system by the Air Products and Chemicals company shows a commercialized state of the art air-oxy/fuel system, whose technology has also been patented under the name US-8696348 B2 since 2007 [24, 25].

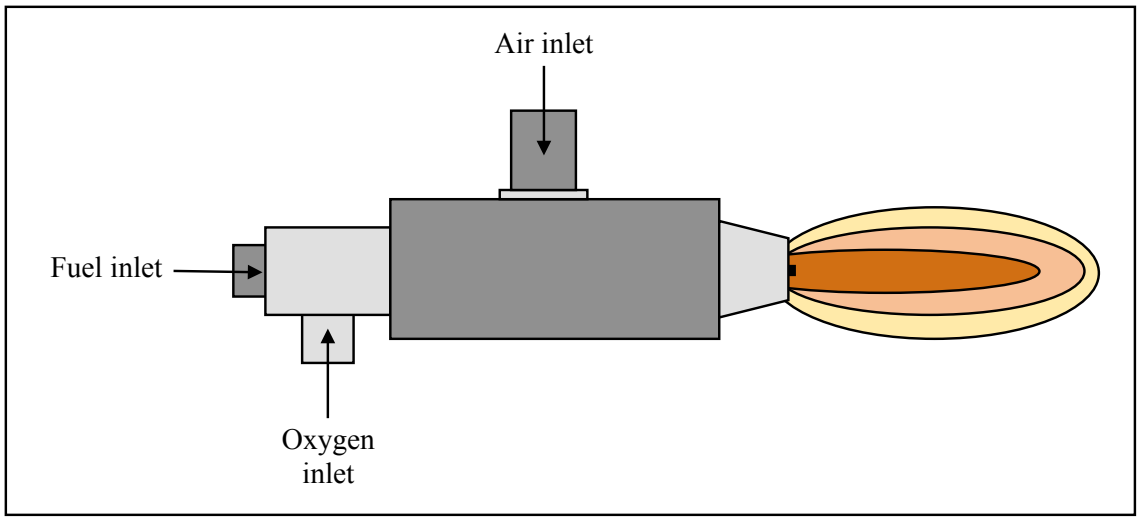

Figure 2.3.: Working principle of an air-oxy/fuel burner

2.6. Oxy/fuel burner systems

Oxy/fuel burners are used in metallurgic processes, especially in iron and steel making industries, over a long period of time. As the industry around aluminum recovery has grown during the past few years, the use of oxy/fuel systems for aluminum recycling have been steadily growing and are spread globally today [23].
The usage of pure oxygen instead of air increases the flame temperature from 2210 °C to 3200 °C, when pure hydrogen is used as a fuel and causes a reduction of the volumetric flow due to the absence of nitrogen, which increases the heat capacity of the gas and may lead to a decreasing fuel consumption [23, 15, 26]. An additional gas recirculation in the furnace can promote energy recovery, as the hot combustion gases can be mixed with the pure oxygen or the fuel. Therefore, individual designs might be used depending on the applied burner. The high temperatures achieved during oxy/fuel combustion are not necessary for melting aluminum but may enhance the thermal efficiency of the process, which may be preferable as an enhanced process performance leads to accelerated smelting time [23, 25]. Another advantage of oxy/fuel burners is that they can be controlled comparatively easy since pure oxygen improves the ignitability of almost every fuel and promotes stable combustion conditions even though fuels with lower heating values are used [23]. All mentioned advantages lead to an outstanding position of oxy/fuel burners for energy intensive applications like metallurgy and are thereby also suitable for aluminum smelting purposes. Furthermore, oxy/fuel burners can lead to zero NO_x emissions, when no fuel bound nitrogen is present and no air is leaking into the system. This fact might be of importance regarding emission limitations for industrial sides, which might become stricter in the future. However, oxy/fuel burner systems require pure oxygen, which needs to be either bought from external suppliers or produced locally. In either case it introduces an additional cost of operation and if produced on site also investment cost. Thus, the installation of such a burner system needs to be evaluated individually. A number of patents for oxy/fuel technology regarding either one specific technological design (i.e. US 5545033, US 5454712) [30, 31] or an overall methodology for oxy/fuel combustion (i.e. US 6596220, US 6436337) [32, 33] are available.

Digression: Production of pure oxygen in industrial scale

In industrial scale, pure oxygen is separated and provided by an air-separation unit (ASU), which is located upstream of the combustion process. To describe the system's working principle briefly, the main operating principle is based on compression of incoming air to make use of the difference in condensing/boiling points of the gaseous compounds found in air. Thereby, the three main air elements nitrogen, oxygen and argon are separated by cryogenic temperature distillation [14].

2.7. Dual-fuel burners

There are two main categories of *dual-fuel burners* distinguished by the types of fuels, gas-liquid and gas-solid [34, 35]. The general differences between the fuel characteristics lead to individual combustion characteristics and with it burner designs [57]. In solid-gas fired burners, solid fine particles (usually coal, or biomass) are fed to the burner via a carrier gas [34, 35, 36]. The carrier gas is usually air for air-fuel combustion and CO_2 for oxy/fuel combustion. It is reported by Sun et al. that co-firing gas with fine biomass particles has shown enhanced heat transfer conditions in the furnace, as the finely dispersed particles enhanced the radiative heat transfer [58]. This increase in radiative heat transfer is likely to occur also for waste-derived fuels, but additional research is necessary to validate this statement. Also the previously mentioned oxidizer lancing principle can be easily adapted for dual-fuel burners (also as a retrofit option) to manipulate the combustion conditions and emissions. The working principle of an air fired dual gas/oil burner is shown in figure 2.4. Regarding fuel feeding, gaseous and liquid fuels is comparatively simple in design, whereas fuel feeding for solid fuels might be very difficult depending on the fuel used. Thus, especially solid fuel feeding needs to be considered in early design phase, as a pre-treatment might be required as the feasible particle size may vary with the burner design and size.

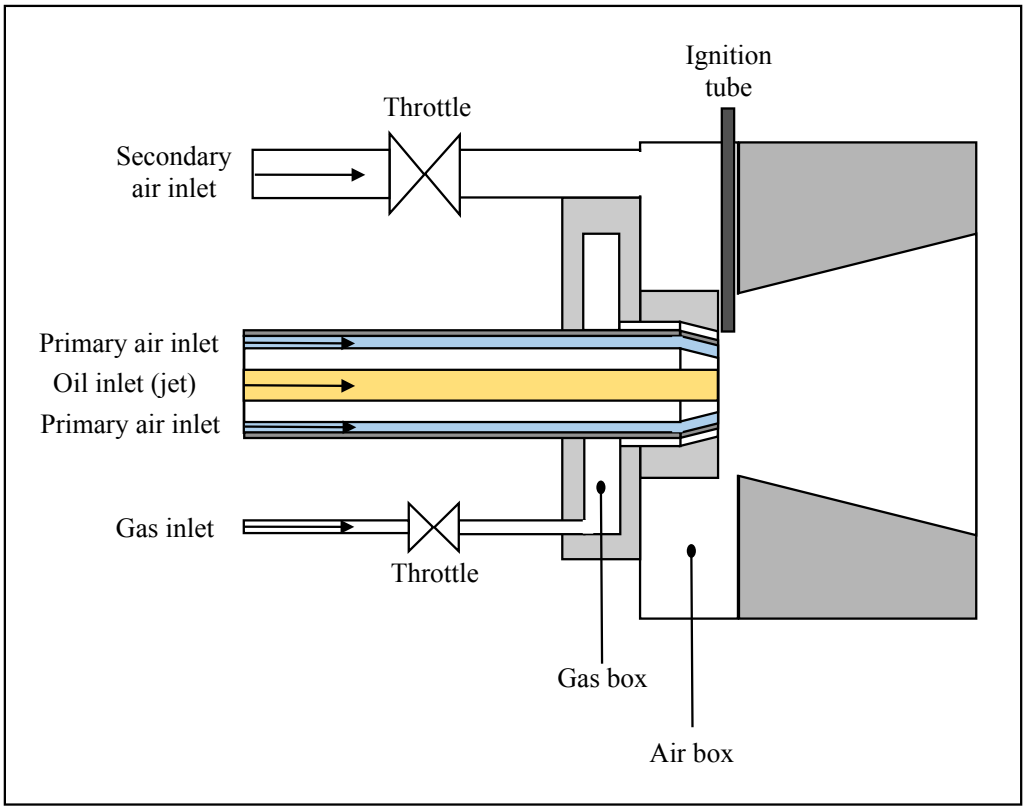

Figure 2.4.: Working principle of a gas/liquid dual-fuel burner system

2.8. Burners in different aluminum smelting furnaces

To start with history, the generic *wet-hearth melting furnace* was in usage for the first half of the 20th century. The technology was very simple in design and handling. Aluminum scrap was charged into the well, which was afterwards shut to start the smelting process. The burner, mounted on the opposite side of the hatchway, heated aluminum scrap up to its melting point. The molten aluminum was simply discharged by using a pump or a closable door at the bottom of the furnace [6, 59, 60]. However, simplicity was favorable during this period of time, technological progress led to other technologies with less limitations. One step forward was taken by the development of the *dry-hearth melting furnace* process, but had still a low thermal efficiency since heat was indirectly transferred from the combustion gases to the aluminum scrap [60].
The first real increase in thermal efficiency was accomplished by the aluminum *stack smelter furnaces*, in which the aluminum has been directly charged into the stack. The scrap has been preheated by hot flue gases leaving the facility, which has enhanced process productivity and has led to energy savings of more than 50 %. On the other hand, the absence of a well has led to a reduction of melt losses up to 80 % as well as emissions, since no slack air has entered the process during charging, an increase of aluminum oxidization has been enabled. A process combination of dry-hearth and stack furnace is applicable and may lead to process advantages which commonly exceed additional investment cost [61, 62]. In further progress, other furnace technologies in combination with other burner technologies (i.e. usage of pure oxygen as an oxidizer

[23]) have obtained market maturity as a totally new technology or a retrofitted existing one [1].

For an overall furnace classification which is based on C.J. Schmitz, three types of furnaces can be regarded. *Hearth furnaces*, also known as reverberatory furnaces, consider the group of furnaces with the largest capacity and the largest diversity, mostly varying between charging spot and shape of the furnace [66]. The furnaces in this group can either have one single chamber or multiple chambers. For example, the Hertwich SMG Group provides single chamber systems with capacities of 10 to 120 tons [64] and multi chamber furnaces with capacities of 30 to 120 tons [65]. The second class is defined as *crucible furnaces*, which differ from the heating technology used (i.e. gas-heated or electrically heated) and show a technological development regarding the hearth furnaces. However, for mechanical strength reasons these furnaces are limited in size and used for smaller volumes (i.e. the LAC company provides capacities for 0.1 - 1.25 tons of Al [63]) [66]. The third class, named *rotary drum furnaces*, mainly consists of the *tilted rotary furnace*, which is going to be discussed in more detail in the upcoming section [66]. This furnace type is considered as a mid small [66] to medium size type with i.e. capacities from 6 to 27 tons (Hertwich SMG)[67] or 12 to 24 tons (Insertec) [68]. Also very small capacities from 0.1 to 2 tons are commercially available [69]. The three overall furnace types are shown in figure 2.5.

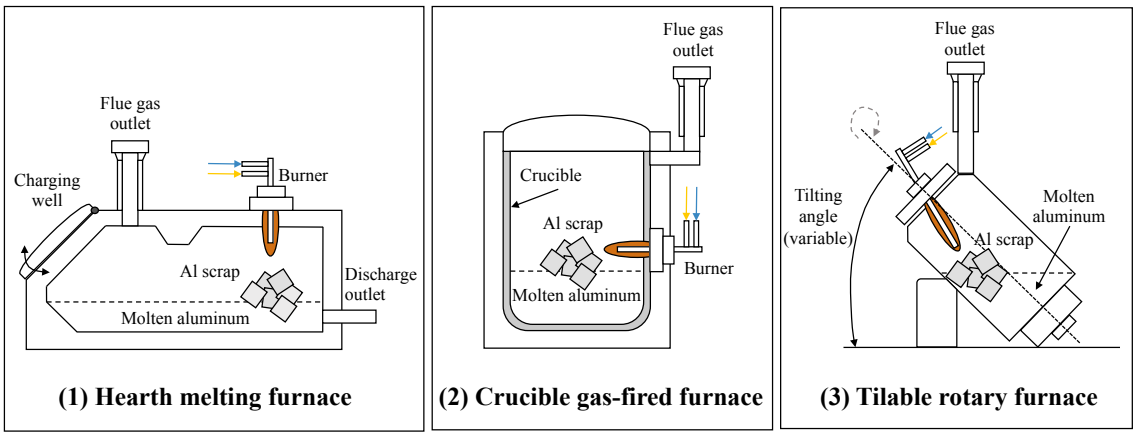

Figure 2.5.: Classification of different aluminum smelting furnace technologies

[1] **Recommended further reading:** Chapter 8-10 "Aluminum Recycling" by M. E. Schlesinger as well as chapter 12.7.1 "Industrial Burners" by Charles E. Baukal

3. Chemistry in combustion

There is not so much information to be found in literature regarding combustion of waste streams such as WEEE which can differ a lot in fuel composition compared to conventional fuels. However, some information can be found. For example there is a report from A. Sepúlveda et al. who has evaluated the formation of some harmful species released from combustion of WEEE. It has been shown i.e., that copper (Cu) acts as a catalyst and enhances dioxin formation during WEEE combustion. The same results have been assessed in a work by M.T. Nguyen et al. [37]. Therefore, it is important to remove as much copper as possible before combustion, not only from a metal recovery point of view but also to avoid additional dioxin formation. When it comes to aluminum smelting in particular, copper can be also introduced together with the aluminum CUPAL (Cu-Al-coating), which can act as an additional source of copper to the system. Additionally, the plastics in electronic equipment and cables as well as automotive residues do often contain brominated fire retardant additives, which tend to form dioxins and furans (PCDD/Fs and PBDD/Fs) as well as other mixed halogenated harmful species (PBCDDs, PBCDFs). Since dioxines and furans have been known to be highly carcinogenic and environmentally harmful, it is necessary to control their formation as much as possible during combustion [83, 37]. In a report from 2006 by J. Brusselers et al. the co-combustion for WEEE at the Umicore Precious Metals Refining plant in Hoboken is investigated [44]. In this test, six weight % of WEEE were co-fired with oil and 3.7 % coke, which was necessary for precious metal processing purposes. It was reported that WEEE co-firing changed heat transfer conditions in the furnace, since it burned earlier above the molten zone. The emissions were reported to not lead to a considerable change, as high temperature (> 1100 °C) could have lead to a destruction of harmful substances. Thus, a co-combustion in this case was not problematic in terms of decreased process performance and/or increased emissions [44].
In addition to the brominated flame retardants found in the plastic part of a.o. WEEE, SLF, cable plastics there is also another halogen found, named chlorine [38, 45]. Chlorine is known to be problematic from a corrosion point of view during combustion as it forms HCl [38, 39]. In a work done by D. Bankiewicz et al. corrosion tests have been made in lab-scale at 1100 °C and 400 °C, and have been compared to ash and gaseous species simulations, containing Na, K, S and Cl and minor amounts of Zn, Pb, Cu, and Br. In the work, 1100 °C was considered to be the approximated combustion temperature in the boiler, and 400 °C the temperature on heat exchanging surfaces, where potential corrosion took place. These temperatures were chosen to represent the combustion of solid recovered fuel (SRF) in a bubbling fluidized bed [40]. As a result of the work, brominated salts led to severe corrosion in a lab-scale test. Another conclusion regarding the main vaporized elements for ash formation. Hereby, S, Cl, Na and K were the main species whereas Zn, Pb and Cu showed minor ash formation behavior.
Processed fuel oil (PFO) has not be in focus of research within the last few years regarding the chemistry of combustion. Some works regarding the fuel gas cleaning after the

combustion of PFO are worth mentioning here, as the results of this works may provide an indication of the combustion behavior and main emissions. A recent work done by S. Gao et al. considers the desulfurization of fuel oils in general but does not consider their combustion and potential pollutant formation [41]. In a work by A. Pawelec et al. a pilot scale electron beam flue gas treatment (EBFGT) plant, located at Saudi Aramco's Refinery in Jiddah, Saudi Arabia is analyzed. Herein, heavy fuel oil fired burners are used with a state of the art highly simultaneous SO_x and NO_x cleaning system, which has shown very high simultaneous removal efficiencies (SO_2 = 98.5%, NO_x = 79.1%). The heavy fuel oil used, is usually applied in industrial boilers and consists essentially of industrial fuels with a sulfur content up to 4% [42].

3.1. Halogen chemistry:

Chlorine is usually released as HCl or chlorinated hydrocarbons, which most often react subsequently to HCl directly after their release [47]. As shown in a work by R. Cossu et al. SLF shows a high risk of corrosion, as a high PVC content leads to a promoted formation of HCl and Cl_2 as well as the formation of toxic dioxins and furans (PCCD, PCDF) [38]. The hydrogen radical H can interact with HCl forming H_2 and Cl as shown in reaction 3.1, or together with the OH radical Cl and H_2O via reaction 3.2, which will diminish CO oxidation [47].

$$HCl + H \rightleftharpoons Cl + H_2 \tag{3.1}$$

$$HCl + OH \rightleftharpoons Cl + H_2O \tag{3.2}$$

HCl interacts with CO indirectly via the set of O/H radicals as shown from a work done by X. Wei et al. There is also an direct interaction with CO as described in reaction 3.3 and 3.4. Thereby, the reaction path following equation 3.4 would promote CO oxidation [47].

$$Cl + HO_2 \rightleftharpoons ClO + OH \tag{3.3}$$

$$ClO + CO \rightleftharpoons Cl + CO_2 \tag{3.4}$$

It should be mentioned, that in traditional fuels chlorine is the main halogen species found, and bromine (Br) and fluorine (F) have then been considered to behave similar as chlorine (Cl). In waste-derived fuels the concentration of bromine and fluorine might not be negligible as eventual differences from chlorine can become important [99, 100, 46]. There is not much to be found in literature about the behavior of bromine and fluorine in combustion. However, some recent experiments have shown that some differences may exist in relation to Cl. For example, Br seems to promote oxidation of mercury to a larger extent than chlorine. This kind of findings suggest that the earlier expected similarity to chlorine could be doubted [97, 98]. For a more precise statement, additional research with focus on bromine needs to be done, as today's upcoming waste-sources (a.o. WEEE, SLF) contain much more bromine than traditional waste-derived fuels (i.e. Municipal Solid Waste) [83].

3.2. Sulfur chemistry:

Sulfur (S) is released to the gas phase mainly in form of H_2S (minor share as CS_2 and COS), under reducing conditions and mainly as SO_2 under oxidizing conditions [47, 40, 48]. As the release form of sulfur does not chance between biomass and solid recovered fuel (a.o. plastics, residential solid waste), P. Glarborg's work for co-combustion of biomass may be also considered. At lower temperatures (< 600 °C) the formation of SO_3 is thermodynamically favored. However, the kinetics are slow and demand for longer residence times to reach an equilibrium that results adequate for a combustion process [47, 48]. SO_2 can also react with free radicals (i.e. OH, HO_2) to SO_3, which can further react with vapor (H_2O) forming sulfuric acid [49]. The main reactions describing the formation from SO_2 to SO_3 are shown in reactions 3.5a, 3.5b and 3.5c. It should be mentioned that SO_2 shows stronger effects under reducing conditions than under oxidizing conditions and, depending on the local oxygen availability, may inhibit or promote CO oxidation [47].
At high temperatures:

$$SO_2 + O(+M) \rightleftharpoons SO_3(+M) \tag{3.5a}$$

At flue gas cool down:

$$SO_2 + OH(+M) \rightleftharpoons HOSO_2(+M) \tag{3.5b}$$

$$HOSO_2(+M) + O_2 \rightleftharpoons SO_3(+M) + HO_2 \tag{3.5c}$$

3.3. Nitrogen chemistry:

Emissions of nitrogen oxides are drawing more attention in today's research as different harmful effects on both the environment and human health are observed. NO_2 is considered to be the most harmful nitrogen species for human health, whereas the nitrogen species N_2O is a harmful greenhouse gas with a 250 times higher effect than CO_2. The formation of NO_2 and N_2O depends on the availability of NO which is most predominating nitrogen oxide species. Thus, a better control of NO emissions may also result in a better control of NO_2 and N_2O emissions.
The reaction rate of thermal NO_x from air present nitrogen increases rapidly with the combustion temperature [53, 51, 52] and considers mainly three reactions, of which the first two reactions were developed by Y.B. Zeldovich in 1946 [54], and the third reaction by G.A. Lavoie et al. in 1970 [55].

Main NO formation reactions:

$$N_2 + O \rightleftharpoons NO + N \tag{3.6a}$$

$$N + O_2 \rightleftharpoons NO + O \tag{3.6b}$$

$$N + OH \rightleftharpoons NO + H \tag{3.6c}$$

Regarding the reaction kinetics for nitrogen active species during combustion (T = 1000 °C) a work performed by R. Edland et al. can be considered, this covers the main pathways form HCN or NO and N_2 (shown in figure 3.1). The work considers a kinetically controlled case as well as a case where mixing conditions dominate the reactions pathways. Herein, HCN is primarily converted into NCO of which a considerable share reacts further to NO (shown in reactions 3.7 and 3.8). Additionally, NH is formed which reacts further to NO and hydrogen regarding reaction 3.9. Nitrogen radicals react preferably to NO when kinetics controlling the chemistry (see reaction 3.10). The work done by R. Edland et al. has shown that NO formation is highly affected by reaction kinetics, as large amounts of NO are formed from NH and NCO.

$$NCO + O \rightleftharpoons NO + CO \tag{3.7}$$

$$NCO + O_2 \rightleftharpoons NO + CO_2 \tag{3.8}$$

$$NH + O \rightleftharpoons NO + H \tag{3.9}$$

$$N + OH \rightleftharpoons NO + H \tag{3.10}$$

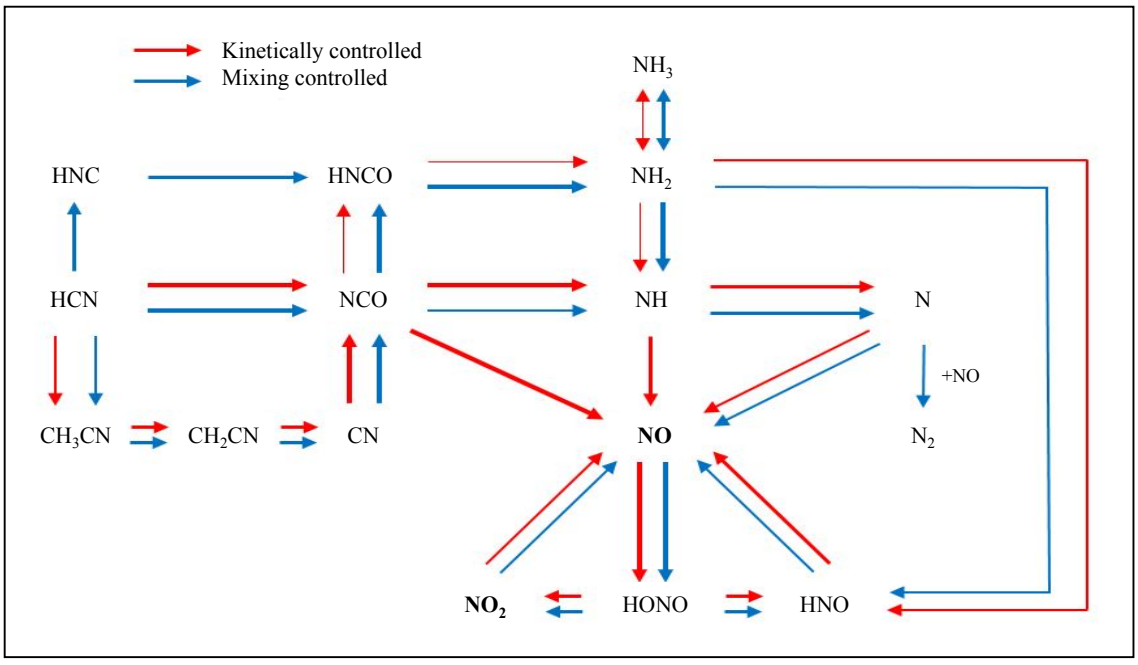

Figure 3.1.: Main reaction pathways from HCN to NO and N_2 [56]

4. The Älmhult process

This chapter provides an overview of Stena Aluminum's smelting process located in Älmult, Sweden, shown in figure 4.1. The combustion part will, however, be described in more detail since this is the focus of this work. It should be mentioned, that the real process differs from the simplified presentation, as for example two universal rotary tilting furnaces (URTF) are used in the real process. After the combustion process in the URTF, a flue gas cleaning system is installed for the removal of particle, chlorine and SO_x as well as an additional afterburner to diminish products of incomplete combustion. When the flue gases leave the URTF, dilution air is added to cool down the hot exhaust gas stream in order to protect the equipment. Thereby, the temperature is regulated to reach 350 °C before the flue gases entering the actual cleaning system. First, the diluted flue gas stream is led through a bicarbonate and activated carbon silo for the removal of sulfur, chlorine and organic compounds, small remaining aluminum particles are captured with a cyclone in order to avoid any damage downstream to the process equipment. Further downstream, the off-gas stream is led through an ash silo for dust removal, before a bag house filter separates the remaining dust. Afterwards, the already particle free exhaust gas stream enters an afterburner unit, which burns off any organic compounds that may still remain at 850 °C. The energy from this additional heating step is exchanged in an economizer unit for heat recovery purposes, in which the heat is transferred to the nearby district heating system, which supplies Älmhult's society. An additional water storage tank with a volume of 800 m^3 exists to regulate variations in the energy flow. The exhaust gas leaves the smelting plant after gas cleaning and heat recovery through a 75 meters high stack, and reaching all necessary environmental emission constraints. The simplified cleaning process can be seen in figure 4.1.

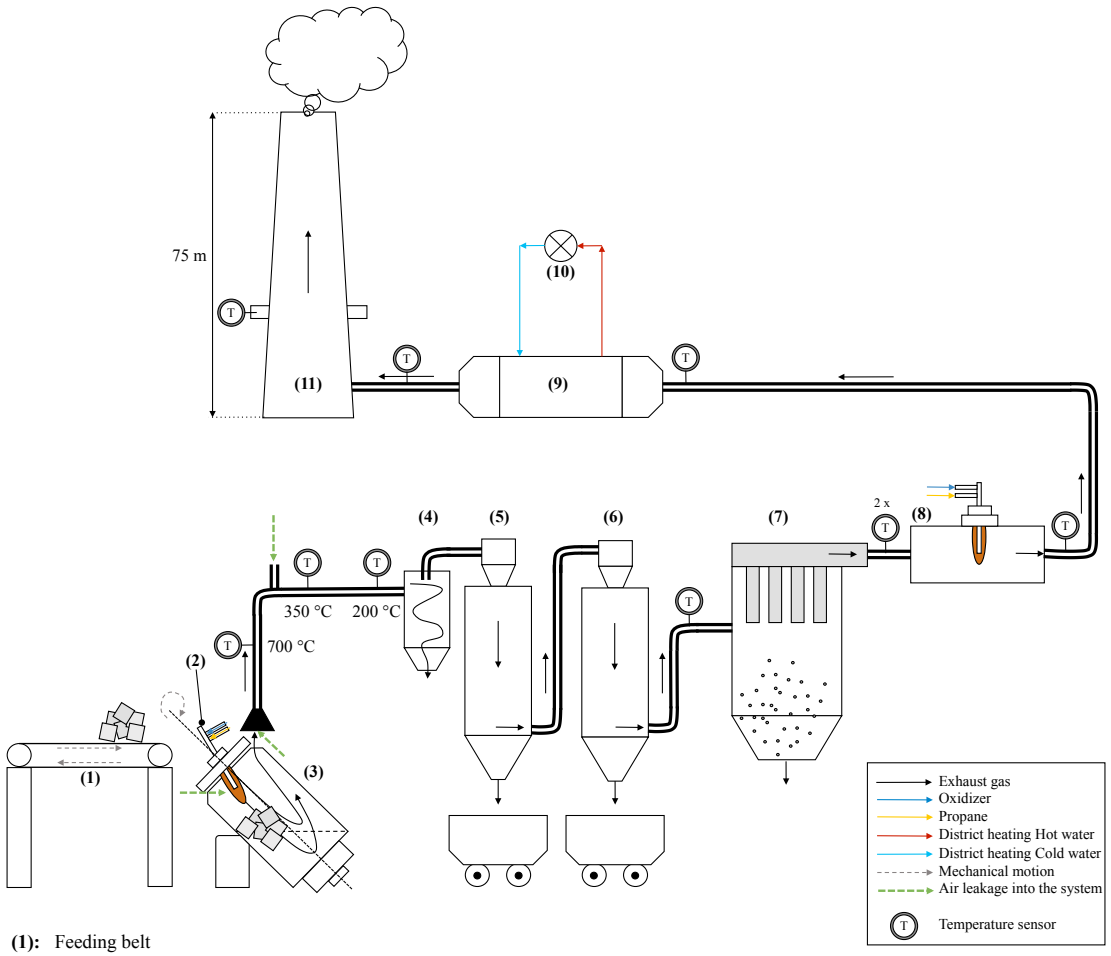

(1): Feeding belt
(2): Oxy/fuel burner (not centered with tilting axis but aligned with Al scrap)
(3): Universal rotary tilting furnace (URTF)
(4): Cyclone to remove small Al particles remaining in the exhaust gas stream, not to damage downstream located equipment
(5): Silo for bicarbonate, which is mixed into flue gas to react with sulfur, chlorine and organic compounds
(6): Silo for activated carbon, which is mixed into flue gas to react with sulfur, chlorine and organic compounds
(7): Bag house filter for separating dust from the flue gas
(8): Afterburner, where organic compounds burned off at 850 ºC
(9): Economizer/ heat exchanger, for heat recovery from flue gas; heat is transferred to the nearby district heating system
(10): Water enters district heating system to supply Älmhult's society; cold water returns to the facility to be reheated
(11): Stack of 75 m height

Figure 4.1.: Process diagram of Stena Aluminum's recycling plant in Älmhult

4.1. The smelting process

Stena Aluminum's recycling facility is a state of the art aluminum recycling plant with a flue gas cleaning system. An aluminum scrap mixture is charged into two large-scale universal tilted rotary furnaces (URTF), fired with an oxy/propane burner. A URTF is a favorable option when aluminum scrap is heavily contaminated with both organic (i.e. introduced with paints, oils, coatings) and inorganic compounds (i.e. hydrogen chlorides, glass, rocks). In combination with air-oxy/fuel or pure oxy/fuel firing system, high combustion temperatures lead to a decreasing melting time as well as lower emissions by a decreasing yield of organic elements of incomplete combustion, which may reduce both fuel and flue gas cleaning costs depending on the previously used process [23]. The

tilting and rotating furnace increases mixing conditions and with it heat transfer, which also reduces melting time and increases aluminum throughput [71]. However, initial investment cost for a URTF may be considerably higher as well as its more complex mechanical design may cause higher maintenance cost [72].
As aluminum is a highly reactive material, especially at higher temperatures, its oxidized and molten form Al_2O_3 has a lower density and floats up at the top of the molten aluminum and this is commonly known as *dross*. The content of metallic aluminum in this dross can vary strongly between 15 to 80 % [1]. As dross occurs as a process loss, or to better say a minimization of the recycling factor (defined as mass of Al scrap input over mass of secondary Al output) it is preferred to keep its formation as low as possible. As an option, secondary aluminum producers, like Stena Aluminum, add an agent to reduce dross generation [1]. As a common standard, a dross flux composition of 50 wt.% NaCl and 50 wt.% KCl is established [75], this may also be used by Stena Aluminum.
The URTF which Stena Aluminum is using is provided by the *Hertwich SMS group*. The systems of Hertwich are highly automatized throughout the whole process from charging to slag tilting, which enables a functional operation with only two operators per shift. To control the combustion (oxy/fuel input), the URTF uses a continuous measurement of CO and temperature in combination with O_2 lancing. Technological development has been leading to very low salt factor of 0.2 [1]. Today, a salt-free system is also available as an ecologically friendly alternative but its application may be a matter of investment possibilities [67].
Furthermore, Hertwich provides a wide range of volumes from 3 to 14 m^3, corresponding to 6 to 27 tons of aluminum scrap per load, of which Stena Aluminum uses the biggest volume available. Melting rates differ between slower rates (1.5 tons/hr) and 6 tons/hr, which is available in Stena Aluminum's system. All available furnaces have a tilting range between -20° and +40°, which varies during operation. Thereby, a tiltback of -20° promotes fast loading. It is also worth mentioning, that nowadays there are more companies providing URTF systems. One example is *Air Products and Chemicals* providing a system under the trademark LEAM (Low Emission Aluminum Melting) [23].
It should be noted, that two URTFs are similar in design but not synchronized in operating conditions, as the quality of aluminum input and output as well as the energy and temperature conditions can differ between both systems. The oxy/fuel burner is provided by *AGA AB* and has an integrated oxygen lance. It is not centered at the kiln's well but aligned onto the scrap / molten aluminum surface to accelerate melting time and enhance offgas circulation.

[1] Salt factor = (amount of salt)/(weight of raw material mix - trial determined aluminium recovery) [70]

Another part of Stena Aluminum's smelting process considers different air leakage flows. Figure 4.2 shows schematically the different air leakage streams into and directly after the furnace. As the charging gate of Stena Aluminum's URTF is not air tight sealed, an unknown air leakage into the combustion process needs to be considered in the reference case evaluation, since this air leakage flow has led to not ideal oxy/fuel combustion conditions but an air/oxygen enriched environment, which results in a considerable NO_x formation in the real process. After the flue gases leave the process, dilution air is used to cool down the temperature to 700 °C (measured at the temperature sensor named T1 in the real process). In Stena Aluminum's process, this dilution air flow is controlled backwards by this temperature sensor T1. For later simulations the dilution air entering the process through the duct and the temperature-controlled gate is summarized to one dilution air flow, called **primary dilution air**. Furthermore, Stena Aluminum's process includes another air inflow entering the process through a "flute" here called **secondary dilution air**. This additional air flow causes a further dilution of the flue gases as well as a further cool down of temperature in the process (down to 350 °C). It should be mentioned, that the considered dilution air flows may not cover the real process to an overall extend, but will however lead to a qualitative evaluation of emissions.

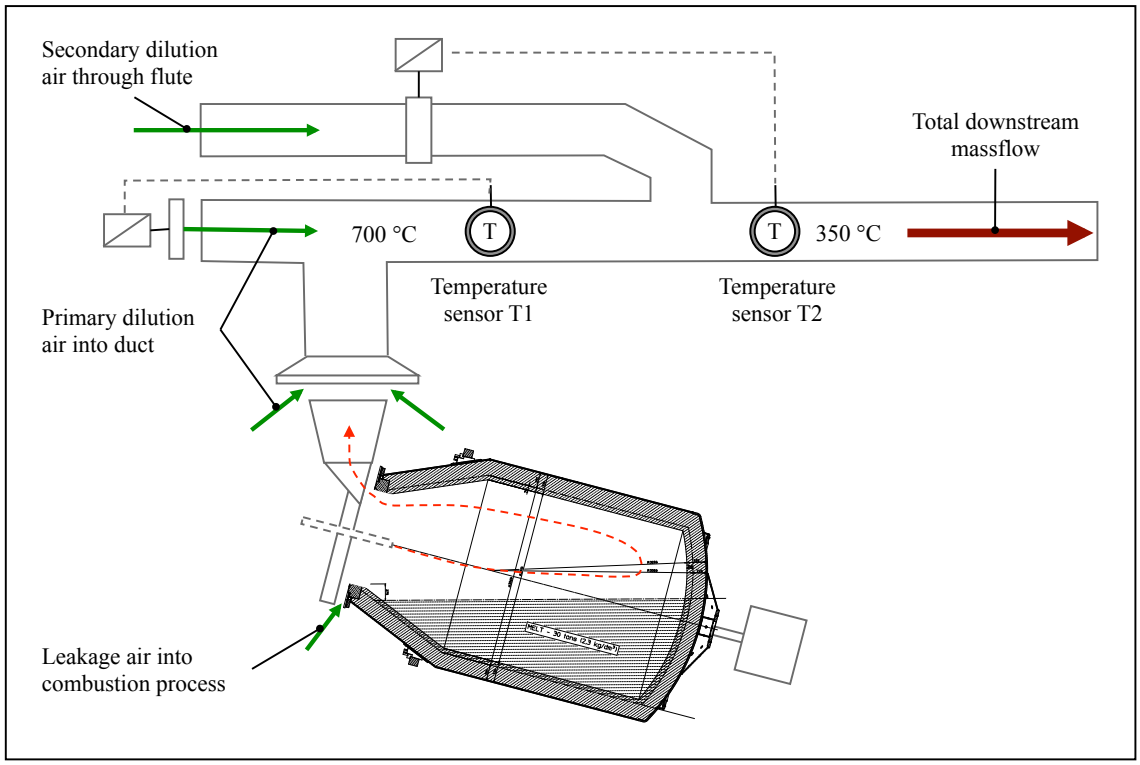

Figure 4.2.: Different air dilution flows in Stena Aluminum's process

4.2. Emission sources and limitations

Some potential emission sources of an aluminum recycling process are going to be mentioned briefly in this section but will not be considered in the later process modeling, which only considers the effects of co-combustion of waste-derived fuels on the combustion related chemistry. However, this chapter gives an overview of potential emission sources which may be considered for future works.

Aluminum scrap: Most likely, aluminum scrap consists of numbers of complex organic compounds, not rarely contaminated by heavy metals. These compounds originate from e.g. paint and other coatings, and contribute to harmful pollutant (i.e. NH_3, unburned hydrocarbons, cyanide, dioxin) formation, and also promote heat delivery into the process. As their concentration differs in every furnace load, special measurement campaigns need to be conducted to investigate their influence in more detail. Stena Aluminum's recycling plant has an activated carbon, a bicarbonate filter as well as an afterburner in order to control the release of unburned hydrocarbons, chlorine and sulfur species. Even though higher emissions arise, using aluminum scrap with a high share of organic compounds, the additional thermal energy directly in the scrap region of the furnace can lead to an enormous reduction of the melting time, which may lead to an increased overall economic process performance, and may therefore be preferred [94]. CFD simulations performed by B. Zhou et al. have shown that the melting time of 13 tons of aluminum scrap in a rotary furnace decreased by 30 %, using scrap with a burn-off rate of 3.5 % instead of pure aluminum scrap without organics (burn-off rate 0 %). Thus, the burn-off rate considers the quality of the aluminum scrap, where scrap with a high burn-off rate is affected by more contaminated scrap with combustible organics [94].
During one batch, temperature conditions change over the time as different exothermal reactions take place which cause a temporary temperature increase. At the beginning of the smelting process, the burn-off of organics in the aluminum scrap appears and causes a temperature increase inside the furnace. Also oxidation of aluminum on the scrap surface increases the surrounding temperature. As these temperature conditions are really unstable over time and may lead to a considerable change in pollutant formation, more stable conditions are chosen for the following simulations in a later stage of the smelting process (after a complete burn-off).

Aluminum oxide: As mentioned in the previous section, aluminum oxide (Al_2O_3) is formed during the smelting process, since aluminum is a highly reactive material. Al_2O_3 follows a spontaneous exothermal oxidation which is slow under ambient temperatures but accelerated with increasing temperatures. Especially, in secondary aluminum production the oxidation process cannot be stopped completely even though a protective salt layer may be present. High temperatures and an oxygen rich environment lead to enhance oxidizing conditions [73]. Thus, aluminum smelters try to control the oxidizer in a way to minimize dross formation [73, 1]. Since Al_2O_3 interactions with other organic and/or inorganic species has not been well researched, some potential future work and a better understanding may improve the process performances and the energy savings.

Oxidation inhibitor: The salt additive which is used to minimize dross formation during the aluminum smelting process contains chlorine (Cl), potassium (K) and sodium (Na). These elements are commonly known to cause a formation of alkaline corrosive salt species. Therefore, additive salts should be considered as a potential emission source, as they are most likely to be partially volatilized, which may lead to an adaption of the fuel gas cleaning system regarding alkaline species. Thus, additional studies have to be performed in order to evaluate the emission contribution.

4.2.1. Emission limitations:

Today's EU emission limitations (mostly NO_x) refer to large combustion plants and power supplier (> 50 MW) and do not consider smaller industrial facilities [78, 79]. For this smaller industrial sites, local authorities have the responsibility for emission limitation. In a directive from the 25th of November 2015, smaller combustion units between 1 MW and 50 MW are addressed with stricter limitations. However, some units are excluded from this directive i.e. "combustion plants in which the gaseous products of combustion are used for the direct heating, drying or any other treatment of objects or materials" [80]. As it is not clear whether this exclusion is valid for aluminum smelting plants, it should only be listed here and may be considered in a later work in more detail. Thus, it depends on the country and the local government, and its assertiveness to what extent environmental restrictions should be and will be fulfilled. The emission limits for Stena Aluminum's process are presented in table 4.1. The table shows the average emission limitations of Stena Aluminum, which need to be fulfilled when running the process. In the future limitations, SO_2 as well as NO/NO_2 are most likely to be imposed.

Table 4.1.: Stena Aluminum's emission limitations

Emissions		
Particles	5 mg/Nm^3	10 ppm
HCl	15 mg/Nm^3	10 ppm
HF	2 mg/Nm^3	3 ppm
Dioxins	0.1 mg/Nm^3	8 ppb
SO_2	75	29 ppm
NO_x	150	120 ppm

Source: [77]

5. Method

Figure 5.1 shows the model used to simulate co-firing combustion of propane and certain fuel alternatives in a universal tilted rotary furnace. The model consists of four different inlets, whereof the inlet for the alternative fuel is excluded for all six reference cases, where only propane is used as a fuel. The propane inlet is used to introduce pure propane into the combustion process. Thereby, the amount of propane (share x_P) depends on the burner power (lower heating value (LHV)), the share of alternative fuel (1 - x_P) and its corresponding heating value used in the process. A more detailed description of the model parts is presented later on in this chapter. It should be mentioned that the presented method is a result of an extensive evaluation process which is presented in appendix C.

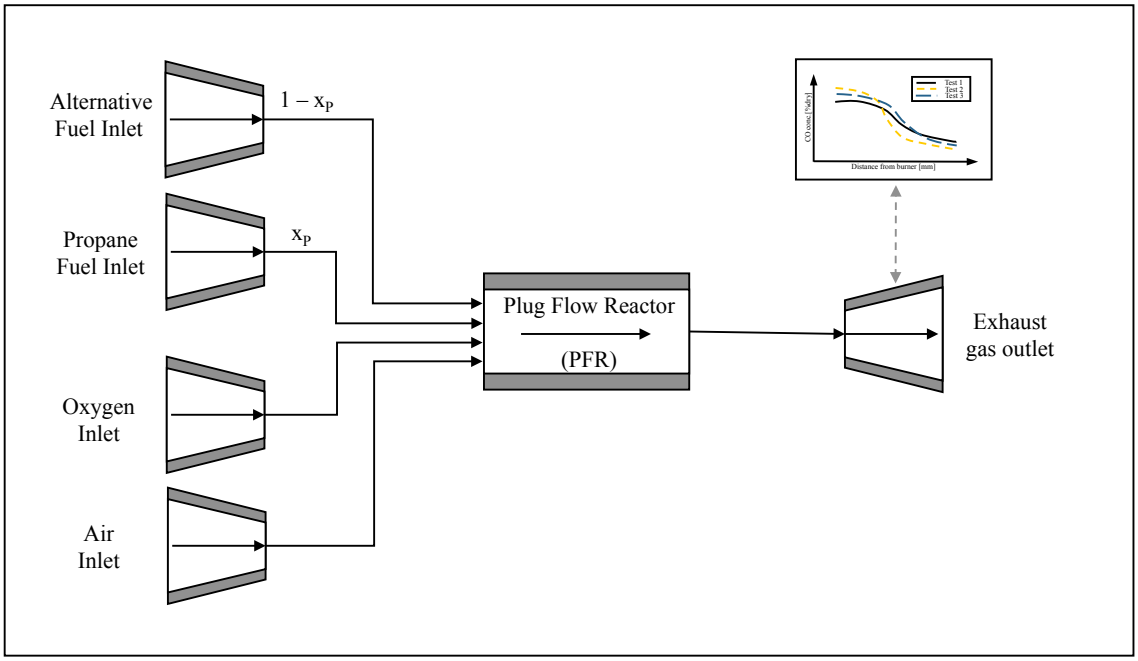

Figure 5.1.: CHEMKIN PRO Model overview

The combustion chemistry was simulated using a plug flow reactor (PFR) model implemented in the software CHEMKIN PRO. This model will only consider the chemical interaction during the combustion of the fuel. Other factors as, furnace titling angle, rotational speed, scrap load and composition are not considered. In a PFR the radial mixing is considered to be ideal which in a real process, like the one here being investigated, is not the case. An oxidizer injection profile, as shown in figure 5.2 (a), is used in an attempt to mimic the reducing conditions found in the flame as a result of mixing resistance. Since Stena Aluminum's URTF has not been sealed, air can flow into the process through the clearance between the rotating furnace pot and the gate. Thus, air is also present in the high temperature combustion zone. Due to this air leakage, the combustion cannot be considered as a pure oxy/fuel combustion but more likely as an oxygen enriched combustion. Furthermore, dilution air is introduced into the process at a later stage, when flue gases leave the furnace into the duct. The air leakage into the furnace and into the duct is represented with an additional air inlet to the model, see figure 5.1. The leakage around the lid is then represented by an air flow of 110 g/s in the beginning and increases logarithmic in the first stage up to 690 g/s to represent the flue gas dilution in the duct. In the second stage, where the dilution air entering the flute is considered, the air flow increases to 5080 g/s. The air injection profile is shown in figure 5.2 (b).

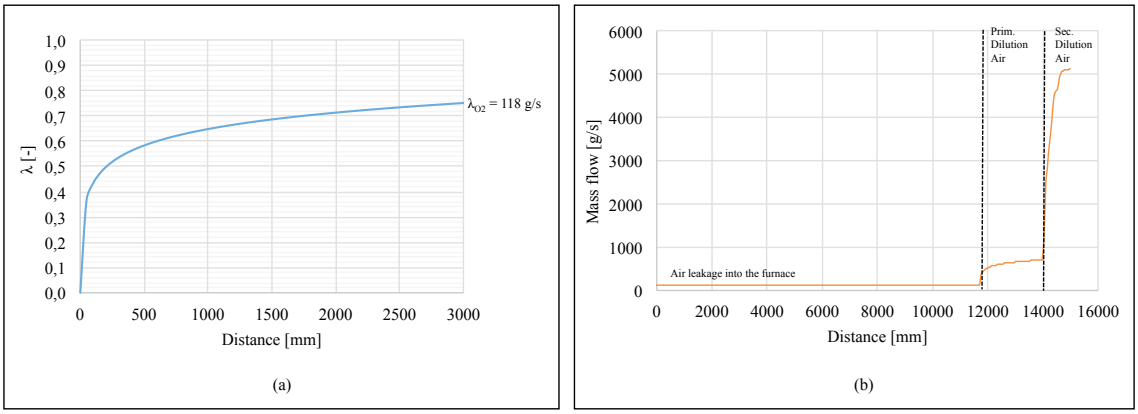

Figure 5.2.: Oxidizer injection profile (a) and air injection profile (b)

It should be mentioned that a total reactor length of 12 meters has been chosen, considering the path length of one gas particle inside the furnace including the turnaround of the gases at 5.3 meter and their way back outside the duct at 12 meter. The calculations considered simple vector algebra and were based on the technical drawing of the furnace, which provided the exact dimensions. After the flue gases leaving the furnace, a mentioned previously two stage dilution is considered form 12 to 14 meter and 14 to 15 meter. A potential particle pathway is shown in figure 5.3.

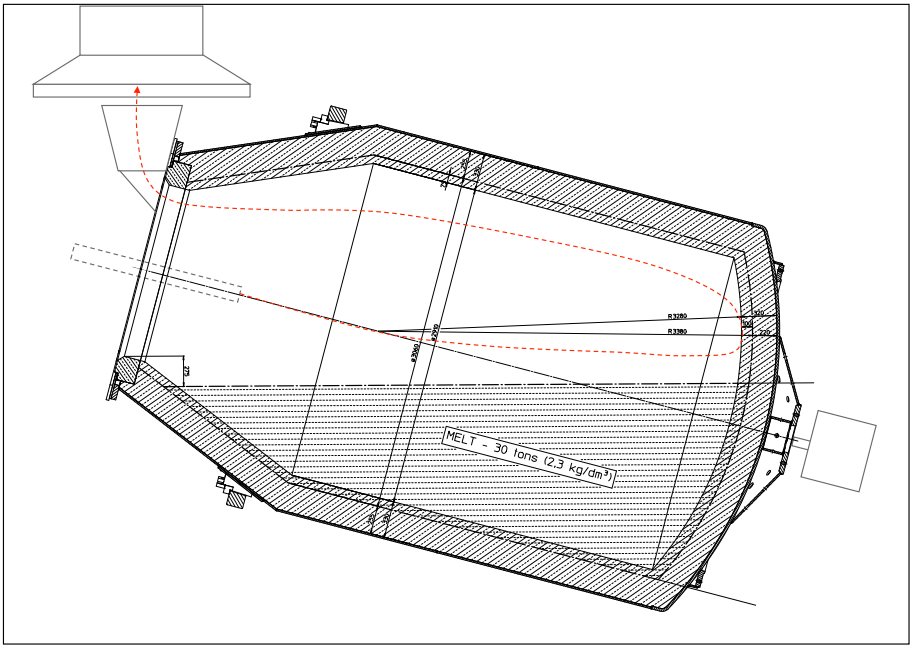

Figure 5.3.: Flue gas flow behavior in Stena Aluminum's URTF

The temperature profile used for the CHEMKIN PRO simulations is based on the results of a CFD simulation of a rotary furnace, which was developed by B. Zhou et al. [94]. The furnace considered in this work has a horizontal design with dimensions of 6.9 meters in length and 3 meters in diameter, which corresponds well with the dimensions of Stena Aluminum's URTF of 5.3 meters in length and 2.91 meters in diameter. Also the burner configuration is similar, as both furnaces are fired with an oxy/fuel burner. The outgoing flow behavior of the off gases in the CFD model differs from Stena Aluminum's process as the CFD model uses a once through furnace, in which the off-gases leave the furnace on the opposite side of the charge gate. In Stena Aluminum's URTF, the flue gases recirculate inside the furnace and leave through a duct mounted on the charge gate, as shown in figure 5.3. The differing flow behavior of the flue gases is adjusted by a slight temperature increase to consider a reheating of the flue gases on their way out of the furnace which is caused by the high temperature combustion zone. The results of the CFD simulation show the high temperature flame zone with temperatures up to 2600 °C, resulting for the combustion of natural gas and pure oxygen [94]. For the temperature profile representing Stena Aluminum's process, this peak temperature is adjusted to 2500 °C for the combustion of propane and pure oxygen. In the results of the CFD model, the temperature inside the furnace around the flame zone is highly uniformed with 1000 °C and goes down to 800 °C when the off-gases leave the furnace [94]. These temperature conditions correlate well with Stena Aluminum's process. The resulting temperature profile is shown in figure 5.3, where five different temperature zones can be seen. The first zone considers the high temperature flame zone, which passes into the burn-off flame zone with a cool down in temperature (zone two). In zone three, the gases hit the bottom furnace wall at 5.3 meter and turn around. Zone four considers the recirculation zone, where gases are slightly heated up again when bypassing the combustion zone, before leaving the furnace at 12 meter (zone five), where they are diluted in two steps and cooled down to 350 °C. The recirculating behavior of the flue gases is shown in figure 5.3.

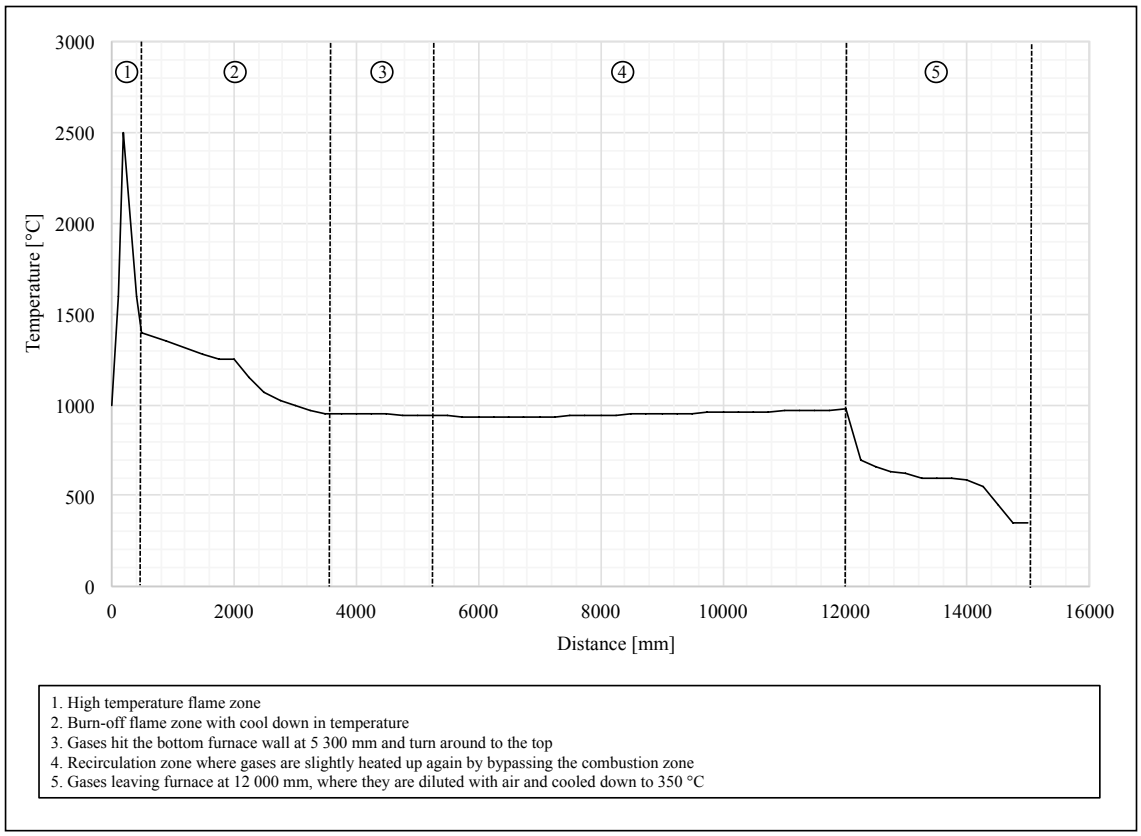

Figure 5.4.: Temperature profile included in CHEMKIN PRO

In addition to the temperature field, the results of the CFD simulations by B. Zhou et al. show a gas velocity profile which is also used in this thesis [94]. The velocity field resulting from the CFD simulations shows "the effects due to the buoyancy force and the furnace geometry" as well as a number of gas flow circles inside the furnace [94]. For this work, the velocity field is simplified into six different velocity zones which are presented in table 5.1. The extracted gas velocity information are numerically translated into a corresponding diameter profile, which is introduced and adjusted in the CHEMKIN PRO software to reach the same gas residence time as theoretically calculated.

Table 5.1.: Assumed gas velocity zones inside Stena Aluminum's smelting furnace

Distance along gas particle path [mm]	**Gas velocity [m/s]**
0 - 300	70
300 - 700	60
700 - 3000[a]	30
3000 - 5300	15
5300 - 12000[b]	5
12000 - 15000[c]	7

[a] Considers a flame length of 3 m, after which no further oxygen is injected.
[b] Gas turnaround point with deceleration due a loss of kinetic energy.
[c] Gases are accelerated through a chimney effect after leaving the furnace at 12 m.

5.1. Reaction mechanism

Different chemistry subsets are covered and implemented in the CHEMKIN PRO software, which are going to be described here. The subset covering halogen and sulfur chemistry was developed by L. Hindiyarti et al. and is explained in more detail in their work [86]. The nitrogen chemistry is covered by different subsets, as different species formations, depending on fuel and oxidizer conditions, need to be considered. The nitrogen chemistry and interaction with oxygen and/or hydrogen are covered by the mechanism developed by P. Dagaut et al. [90]. Additionally, the ammonia chemistry is covered by Skreiberg et al. [91]. Different $C_xH_yO_z$ species and their interactions with nitrogen (N) are, with exceptions, covered with a mechanism developed by C.L. Rasmussen [92] and P.Glarborg et al. [93]. Whereas the reaction kinetics of a carbon monoxide CO / NO_2 interactions are covered regarding [85] as well as the interaction of CO / N_2O by [91]. The propane (C_3H_8) chemistry is covered in a subset developed by P. Glarborg et al. The same author also developed the C_1 and C_2 oxidation subset, included in the executive CHEMKIN PRO mechanism [85].

5.2. Transformation of alternative fuel into fuel gas

There are seven different fuels investigated in this work for the purpose of co-combustion with propane, see table 5.3. The software CHEMKIN PRO that is used in this work only considers gas phase reactions for those species that are defined in the reaction mechanism. The fuel composition (see appendix A for complete composition analysis) therefore has to be converted to a representing fuel gas that can be used as an inlet to the simulation. The method for converting the real fuel composition is summarized in table 5.2. Additionally, it should be additionally mentioned that all bromine (Br) and fluorine (F) are assumed to behave as chlorine (Cl), and the introduced amount of Cl is therefore the sum of Cl, Br and F. The form in which the different elements are introduced into the model can be seen in table 5.2. As presented, carbon is introduced as CO. However, the amount of oxygen available in the fuel is not sufficient to convert all carbon into carbon monoxide

(CO). To keep the overall mass balance, the additional oxygen added is subtracted from the oxidizer. Additionally, a moisture content for each fuel is introduced with the fuel gas as H_2O. The moisture content, given on a total mass basis is thereby transformed into a weighted share of H_2O on a fuel gas weight basis. More detailed calculations to transform the elementary fractions into a fuel gas used for CHEMKIN PRO can be found in appendix B. It should be mentioned that the composition of cable plastics and PUR is based on a pyrolyzed gas, which has been dechlorinated before the pyrolysis.

Table 5.2.: Transformation of alternative fuel fractions into fuel gas

Elementary analysis	**CHEMKIN PRO fuel gas species**
C	$\rightarrow$ CO
H	$\rightarrow H_2$
S	$\rightarrow H_2S$
N	$\rightarrow$ HCN
Cl	$\rightarrow$ HCl
F $\sim$ Cl	$\rightarrow$ HCl
Br $\sim$ Cl	$\rightarrow$ HCl
Moisture	$\rightarrow H_2O$

The resulting weight shares for the fuel gas, introduced in the CHEMKIN PRO model, are summarized for each fuel in table 5.3 and presented in $\%\ {}^{g_x}/_{g_{Fuelgas}}$. Also the LHV for the fuel, its ash content as well as the required amount of oxygen per MJ of fuel is presented, assuming a stoichiometric fuel combustion.

Table 5.3.: CHEMKIN PRO fuel gas weight shares for alternative fuel

Alt. fuel	**C_3H_8** [%]	**CO** [%]	**H_2** [%]	**H_2S** [%]	**HCN** [%]	**HCl** [%]	**H_2O** [%]	$\left[\frac{MJ}{kg_{fuel}}\right]$	$\left[\frac{g_{O_2}}{MJ}\right]$	**Ash** [$\%_{wt}$]
Cable	-	94.0	5.65	0.001	0.08	0.10	0.14	32	74	14
PUR	-	86.1	2.40	1.30	7.14	0.64	2.48	15	162	50
$WEEE_{In.}$	-	86.7	3.22	0.01	1.62	1.02	7.43	30	69	6
$WEEE_{LF}$	-	84.4	3.82	0.09	3.22	5.84	2.67	20	102	24
SLF	-	84.5	4.53	0.31	1.91	1.32	7.41	14	132	45
Rubber	-	97.6	1.36	0.53	0.12	0.02	0.40	32	84	9
PFO	-	93.3	5.96	0.37	0.11	0.07	0.20	41	80	0.8
Propane	100	-	-	-	-	-	-	46	79	-

5.3. Reference case

The selected reference case considers higher air availability inside the furnace (leakage air) but substoichiometric conditions regarding pure oxygen feeding, which corresponds well with Stena Aluminum's process conditions. Furthermore, the overall stoichiometry inside the furnace is kept constant at $\lambda_{Furnace} = 0.9$ for all co-firing simulations. Therefore, the oxygen profiles has to be adapted for each fuel alternative, since different oxygen

requirements per MJ lead to different behaviors compared to a pure propane combustion. For all fuel alternatives, the co-firing simulations are made regarding a power of 2 MW for the burner, fired by **60 % of propane** and **40 % of alternative fuel** on an energy basis (regarding LHVs). Thereby, the average temperate is chosen to be 950 °C inside the furnace with a peak combustion temperature of 2500 °C. The dilutional effects are adjusted to reach similar CO_2, H_2O and NO outgoing concentrations as measured from Stena Aluminum. Thus, it can be assumed that Stena Aluminum's process is represented to a valuable extent.

5.4. Sensitivity analysis

To cover different uncertainties resulting from assumptions during the model setup, a sensitivity analysis is performed with respect to five parameters. An overview of the regarded sensitivity analysis is summarized in the following listing:

- Isothermal temperature conditions
- Peak combustion temperature (1. zone figure 5.4)
- Average furnace temperature (2. and 3. zone figure 5.4)
- Residence time
- Oxygen availability during combustion

The sensitivity analysis, which investigates the effect of isothermal temperatures, considers 80 different temperatures between 700 °C and 2300 °C, and their effect on the outgoing pollutant concentration before dilution air enters the process. In the sensitivity analysis where the peak combustion temperature is changed (1. section figure 5.4), two simulations with a high peak combustion temperature of $T_{\text{Peak}} = 2500°\text{C}$ and a lower peak combustion temperature of $T_{\text{Peak}} = 2000°\text{C}$ are made. Also the effect of the average temperature inside the furnace is considered in a sensitivity analysis, wherefore one simulation with a high average furnace temperature of $T_{\text{Average}} = 1100°\text{C}$ and one with a lower average temperature of $T_{\text{Average}} = 800°\text{C}$ is performed (2. and 3. zone figure 5.4). The effect of the residence time and with it the uncertainty of the considered gas velocity field is covered by changing the residence time inside the furnace for each considered fuel between 0 and 25 seconds, wherefore 160 intervals are considered. Another sensitivity analysis covers the residence time directly in the high temperature combustion zone, where the residence time is varied by ± 15% for each fuel.
In the co-firing simulations, substoichiometric conditions were used ($\lambda_{\text{Furnace}} = 0.9$), as to represent the conditions in Stena Aluminum's process. To cover the uncertainties of these stoichiometric conditions, a sensitivity analysis is performed considering eight different air-to-fuel equivalence rations λ_{O_2} between 0.5 and 3 (λ_{Furnace} 0.65 and 3.15).

5.5. Alternative fuel selection

The selection criteria for different alternative fuels with a high potential of co-firing with propane in Stena Aluminum's recycling facility follows two main steps. The co-firing simulations with all seven fuel alternatives should provide the base for the first selection step, where three fuels are going to be chosen for further sensitivity analysis. Especially, the simulated NO_x, SO_x and halogen emissions are going to be considered in the fuel selection. A second selection step is not only going to consider the results of the sensitivity analysis of the three previously selected fuels, but also their yearly availability, oxygen requirement and ash composition, which may all together result in one preferable waste-derived fuel co-combustion in Stena Aluminum's recycling facility.

6. Results

The alternative fuels suggested for co-combustion in Stena Aluminum's facility in Älmhult have been evaluated via the combustion modeling. Each of the fuels has been combusted together with propane in a ratio of 4/6 on an energy basis. The results are then compared to combustion of 100% propane. As it can be seen in figure 6.1, all fuels show similar profiles with respect to both CO and CO_2 and differ only in absolute values. The simulated CO_2 concentration inside the furnace, shown in figure 6.1b, varies between 25% (pure C_3H_8) to 28% (PUR) for the different fuels. Among the alternative fuels cable plastic shows the lowest CO_2 concentration. However, after dilution the concentration does not differ to any significant extent between any of the eight cases investigated. It is clearly visible that the combustion for all co-firing options is incomplete inside the furnace since there is a noticeable CO concentration present at the furnace exit, see figure 6.1a. The CO concentration at this point varies between 1% (PFO) and 5% (Pure Propane).

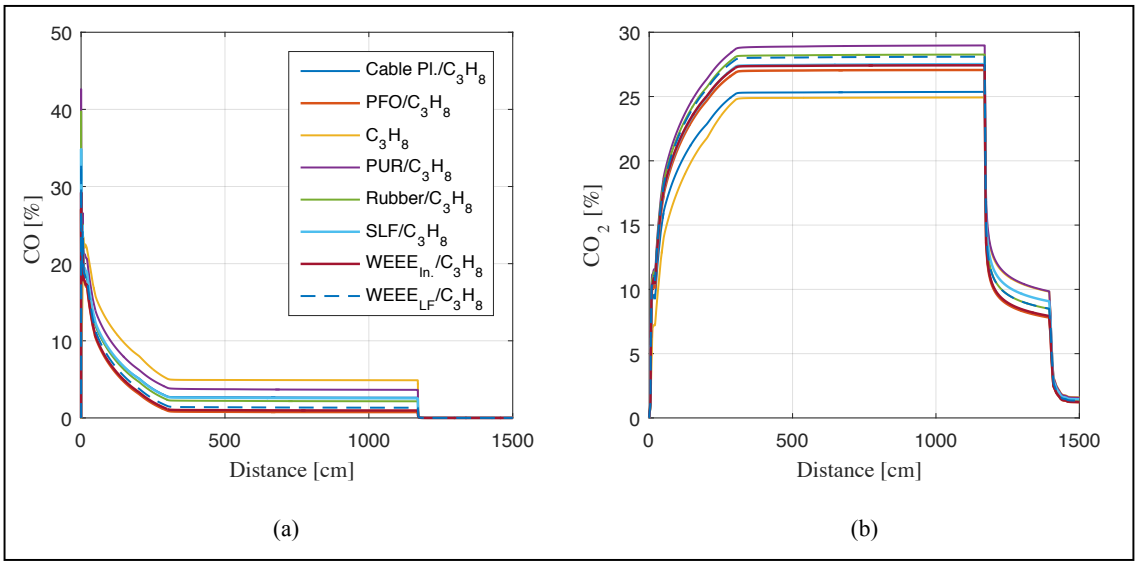

Figure 6.1.: CO, CO_2 concentration for co-combustion of different alternative fuels compared to the reference case where pure propane is combusted.

Figure 6.2 shows the concentration of NO and NO_2 for all regarded fuel alternatives. The NO concentrations (figure 6.2a) show similar behaviors between the different co- firing fuels, whereas absolute numbers are varying depending on the chemical composition. With an increased HCN concentration in the fuel gas an increasing NO formation can be regarded. A NO peak for all fuels is reached at peak combustion temperature, which corresponds to known NO behavior during combustion, as thermal NO is most likely to be formed at high temperatures where fast reaction kinetics occur. After reaching the peak, NO is diluted by the additional oxygen entering the system until it stabilizes after 300 cm, where no further oxygen is introduced. PUR shows the highest concentration of NO with 1400 ppm inside the furnace as well as the highest outgoing concentration with 48 ppm after full dilution. Cable plastics show both the lowest NO concentration among all co-firing options (330 ppm inside the furnace) and lowest HCN concentration of the fuel gas. PFO and Rubber show a similar HCN concentrations in the fuel gas, which results in a similar NO_x behavior. SLF and $WEEE_{Inc.}$ also show a similar NO behavior (720-740 ppm inside the furnace) whereas $WEEE_{LF}$ shows a higher NO concentration with 880 ppm.
The comparison of NO_2 shows its formation mainly at lower temperatures, figure 6.2b. Differing in absolute numbers, the co-firing fuels follow the same pattern.

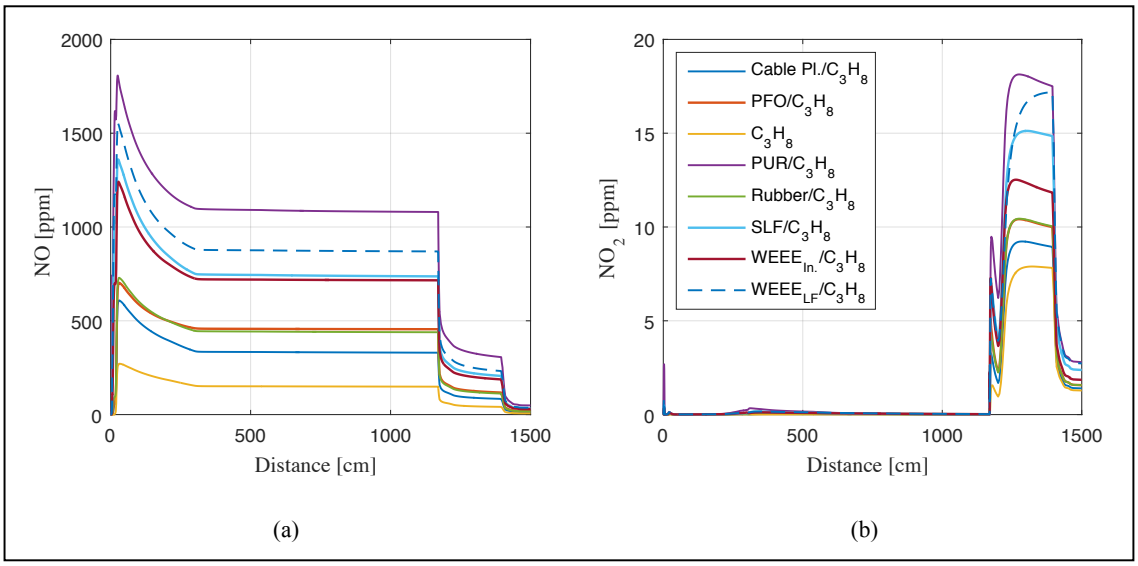

Figure 6.2.: NO, NO_2 concentration for co-combustion of different alternative fuels compared to the reference case where pure propane is combusted.

The Cl and HCl profiles for the different alternative fuels are shown in figure 6.3. The chlorine radical Cl is formed similar to the oxygen radical O at high temperature and additionally when dilution air is introduced, shown in figure 6.3a. After Cl formation the radicals re-react to HCl and other chlorine species. It can be seen that the highest Cl peak concentration is reached for $WEEE_{LF}$ when the combustion temperature reaches its maximum of 2500 °C, as this fuel has the highest chlorine content. The chlorine concentration for PUR is slightly higher than for $WEEE_{Inc.}$. The HCl concentrations shown in figure 6.3b have mostly shown an individually constant behavior inside the furnace for each fuel, with concentrations between 9.7 ppm for Rubber and 3741 ppm for $WEEE_{LF}$. The lowest outgoing HCl concentrations after dilution were reached for Rubber (0.4 ppm) and PFO (1.5 ppm), whereas the highest concentration was reached for $WEEE_{LF}$ (169.7 ppm).

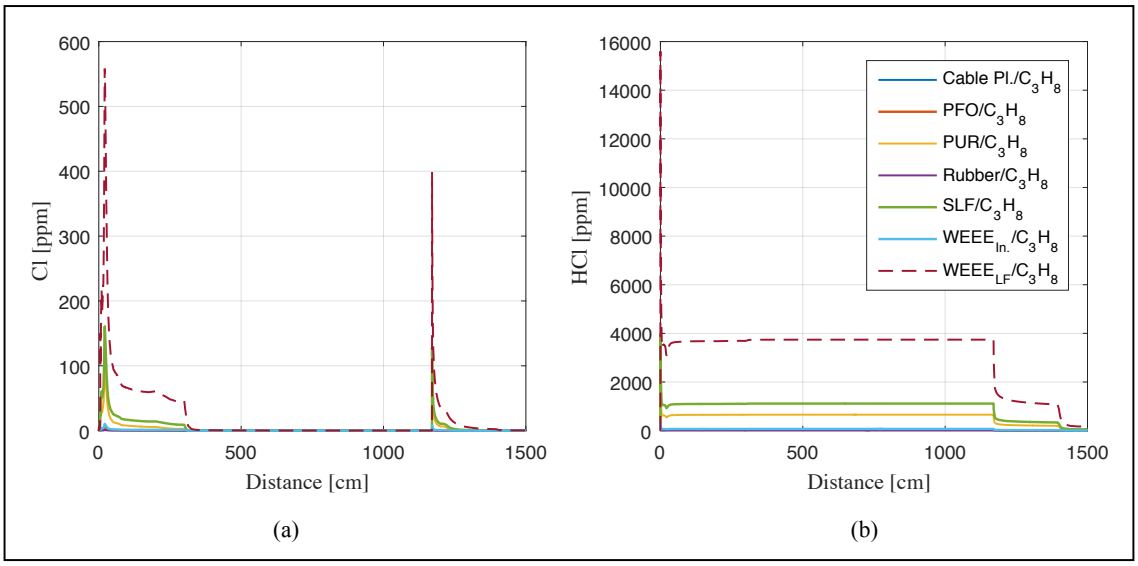

Figure 6.3.: Cl, HCl concentration for co-combustion of different alternative fuels

The lowest SO_2 concentration inside the furnace was simulated for cable plastics with 0.5 ppm as shown in figure 6.4a. The highest SO_2 after dilution was, on the other hand, reached for PUR and Rubber, with 1415 ppm and 460 ppm respectively. PFO has shown a SO_2 concentration of 187 ppm inside the furnace, but decreases with dilution down to 8 ppm. It should be mentioned, that sulfur was introduced as H_2S with the fuel gas, but is decomposed after 5 cm for all fuel alternatives to other sulfur containing species. SO is formed at high temperatures and high availability of oxygen and follows the O radical availability. SO_2 shows, especially at high temperatures, an inverse behavior to SO. When SO is decomposed it reacts to SO_2. Thus, the SO concentration is decreasing, whereas the SO_2 is increasing.
SO_3 is most likely to be formed when dilution air enters the system as more oxygen is available, seen in figure 6.4b. The higher the sulfur concentration in the fuel the more SO_3 is potentially formed. Thereby, PUR reaches the highest outgoing concentration of 1.6 ppm, whereas $WEEE_{Inc.}$ and $WEEE_{LF}$ show the lowest SO_3 concentration. Also PFO has a low SO_3 concentration of around 0.20 ppm after dilution.

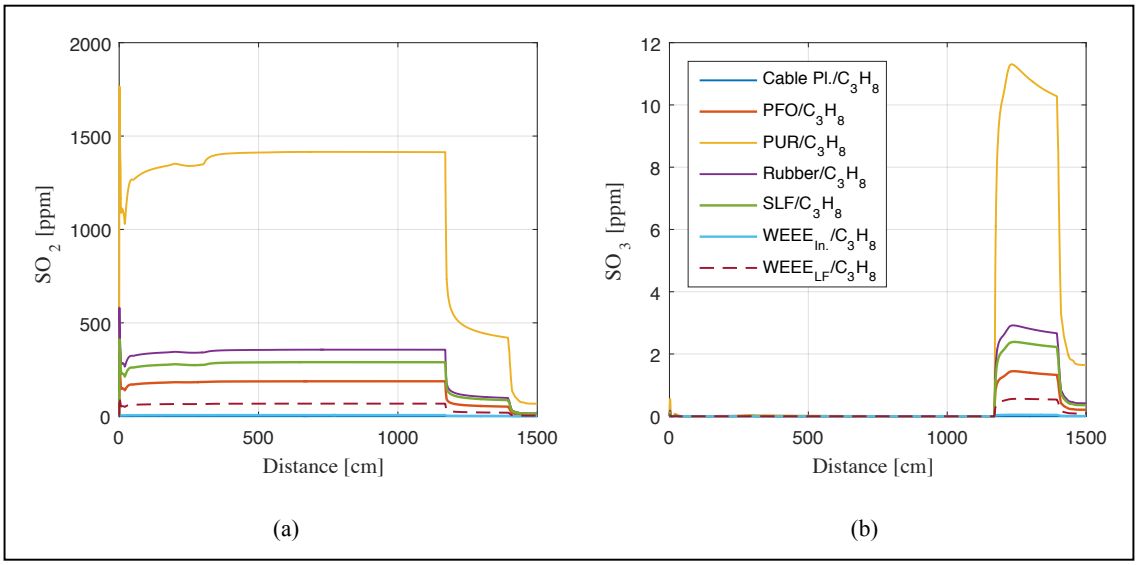

Figure 6.4.: SO_2, SO_3 concentration the co-combustion of different alternative fuels

6.1. Sensitivity analysis

The sensitivity analysis is performed with three waste-derived fuel as potential co-firing options. The selection of this fuels is based on the argumentation included in the discussion and can be found in chapter 7.

6.1.1. Temperature

Figure 6.5 shows the concentration of NO, HCl and SO_2 versus temperature. NO formation showed an exponential increasing behavior with increasing temperature, starting over 1600 °C as shown in figure 6.5a, whereas NO_2 was formed at temperatures between 700 °C and 1100 °C, where a peak is reached around 760 °C. N_2O followed the same pattern as NO_2, but both results are not presented here. The results for nitrogen follow the theoretical NO_x formation behavior are presented previously in this work. As it can be seen in figure 6.5b, HCl shows a decreasing behavior starting over 1200 °C, as HCl is decomposed to Cl radicals. Between 740 °C and 780 °C it shifts first to Cl radicals, which is not presented here, with a later reformation to HCl can be regarded, and explains the jumping HCl behavior in this temperature interval. SO_2 formation, presented in figure 6.5c, showed a slightly increasing behavior with a peak at around 1700 °C. SO_3, showed a formation peak at a temperature of 950 °C in the temperature interval of 760 °C to 1700 °C. SO showed a similar formation behavior as NO, starting over 1600 °C, but is not presented here. It should be mentioned that the absolute number may vary in reality, but should follow the overall trends.

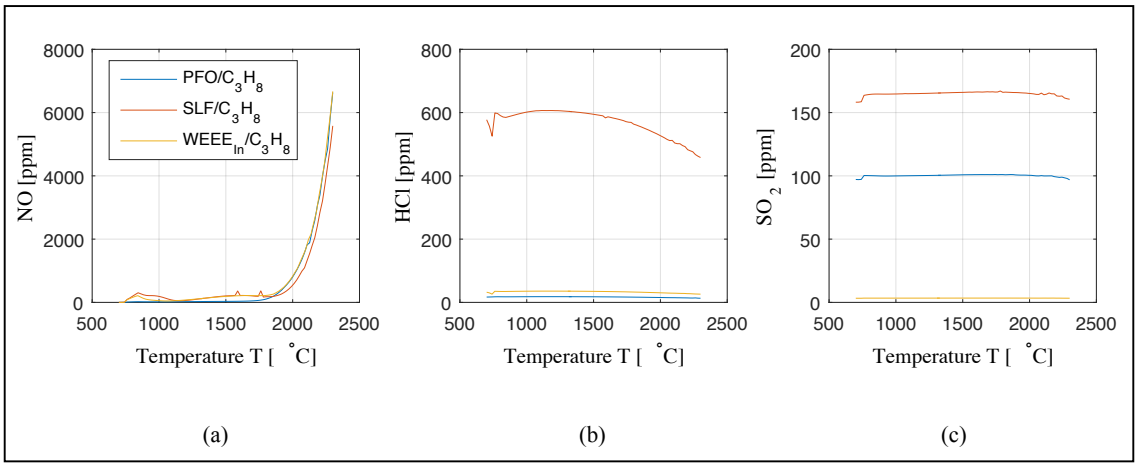

Figure 6.5.: Temperature versus concentration of selected pollutants

Changing the peak combustion temperature, as shown only for PFO in figure 6.6, led to increasing NO formation (figure 6.6a) at a higher peak combustion temperature for all three regarded fuels and with it to an increasing formation of NO_2 and N_2O. Also SO was slightly higher at a higher peak temperature which resulted in a slightly higher SO_2 formation (figure 6.6c). SO_3 formation before dilution was slightly increased but decreased after dilution.

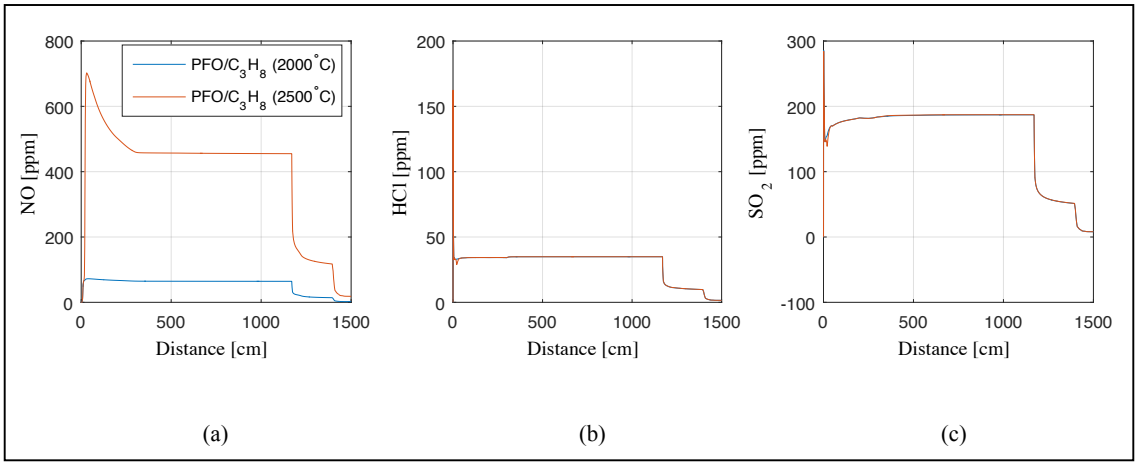

Figure 6.6.: NO, NO_2, SO_3 conc. at different peak combustion temperatures

The effect of changing the average temperature is shown in figure 6.7. The figure only shows the results for PFO because the other fuels follow the same trend. A higher average temperature led to an increasing NO concentration (figure 6.7a), whereas the NO_2 and also N_2O concentration (not included in the figure) showed an increasing behavior at a lower average furnace temperature. No considerable change of SO, HCl (6.7b) and SO_2 (6.7c) formation were observed.

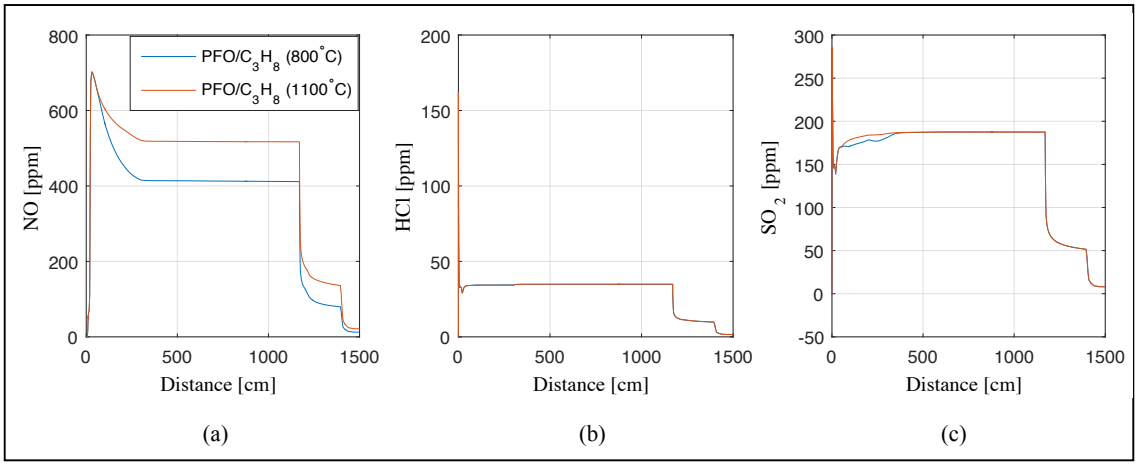

Figure 6.7.: NO, HCl, SO_2 conc. at different average furnace temperatures

6.1.2. Residence time

The results are presented for PFO co-firing only since the other fuels included in the sensitivity analysis followed the same overall behavior differing only in absolute numbers. NO (figure 6.8a) showed a formation peak around 0.7 seconds. NO_2 showed a concentration peak at a residence time of one second. For residence times over one second the concentration of NO_2 showed a decreasing behavior going down to almost 0 ppm for residence times over 10 sec. The same behavior was observed for N_2O formation with a formation peak at around one second. For a longer residence time only in the high temperature combustion zone, more NO formation was observed but is not presented here. HCl (figure 6.8b) showed a lower formation for really short residence times but increases with a logarithmic behavior before reaching almost constant values for residence times over 1.5 seconds. Cl showed an inverse behavior, with high concentrations for really short residence times and a rapid decrease for longer residence times. Furthermore, SO_2 (figure 6.8c), as well as SO_3, showed a similar behavior to HCl with first a rapid increase and an afterwards constant behavior over 1.5 seconds. SO showed an inverse behavior similar to Cl.
For longer residence times in the high temperature combustion zone, increasing NO peak concentrations for PFO and $WEEE_{Inc.}$ were observed. SLF showed the same peak concentration but a lower NO concentration inside the furnace. This result is controversial with the behavior of PFO and $WEEE_{Inc.}$, and may be explained as SLF has the highest HCN content and at the same time the lowest LHV, which leads to an increasing mass flow of SLF to provide the same amount of energy. The sulfur and chlorine chemistry were not affected by changing the residence time inside the high temperature combustion zone.

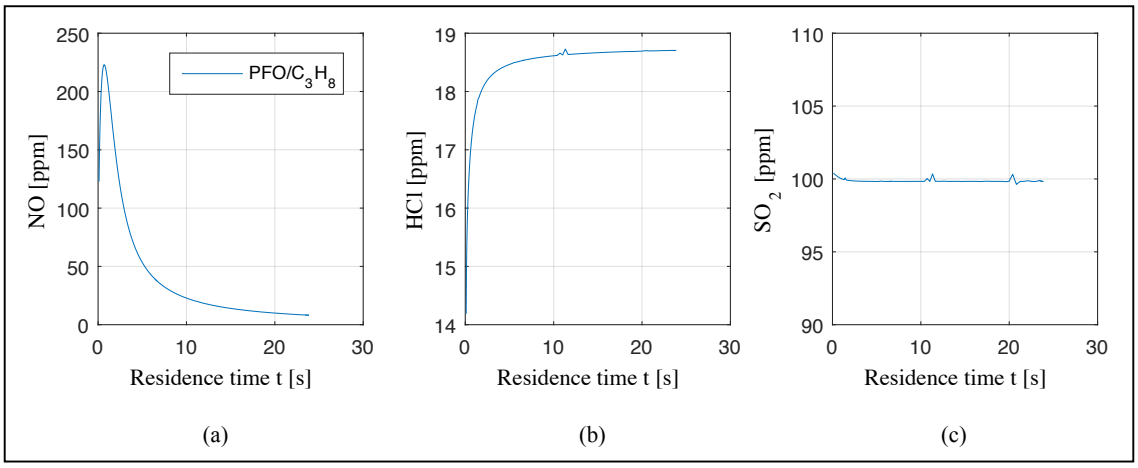

Figure 6.8.: Residence time versus concentration of selected pollutants

6.1.3. Oxygen availability

In order to have a much better understanding, only the behavior of PFO is shown in figure 6.9, as the other two considered fuels (SLF, $WEEE_{Inc.}$) showed the same behavior, differing in absolute numbers. Thereby, the concentration inside the furnace before dilution for NO, HCl and SO_2 is presented over the air-to-fuel equivalence ratio λ_{O2}. The NO concentration, figure 6.9a, showed a highly increasing behavior with an increased oxygen availability and peaked around $\lambda_{O_2} = 2.0$. NO_2 showed the same pattern with a peak at around $\lambda_{O_2} = 2.0$. N_2O showed a maximum at $\lambda_{O_2} = 0.75$, a minimum at $\lambda_{O_2} = 1.0$ and increased afterwards with increasing λ_{O_2}. HCl formation, figure 6.9b, showed a decreasing behavior with increasing λ_{O2}, but no changing in shape regarding the co-combustion simulations was observed. Less SO was formed for $\lambda_{O_2} = 0.5$ compared to $\lambda_{O_2} = 3.0$. The SO_2 formation (shown in figure 6.9c) showed a peak at $\lambda_{O_2} = 0.75$ and decreased afterwards. SO_3 increased rapidly with reaching a maximum around $\lambda_{O_2} = 1.5$. Afterwards a smoother decrease was observed. Additionally, a dependence on temperature was investigated for the slope of the SO_3, where the gradient was increased with decreasing temperature and almost constant inside the furnace before dilution.

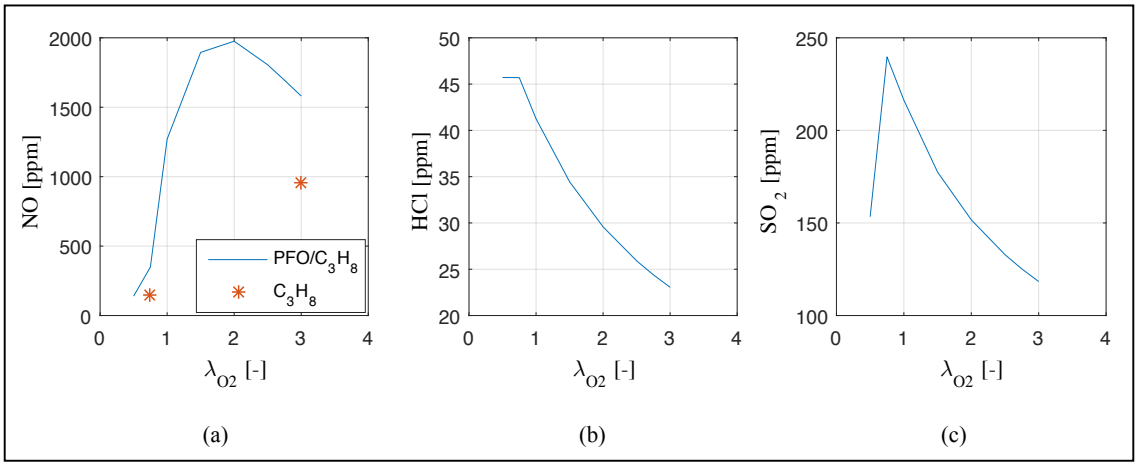

Figure 6.9.: Stoichiometry versus concentration of selected pollutants

7. Discussion

The focus of this work lied on the evaluation of a suitable waste-derived fuel for a co-combustion together with propane in Stena Aluminum's recycling facility located in Älmhult, Sweden. As a part of this evaluation, CHEMKIN PRO simulations with seven different waste-derived fuels were performed and showed residence times between 1.4 and 1.7 seconds, varying with the volumetric gas flow for each waste-derived fuel.
According to the presented results, PUR showed the highest NO concentration with 1100 ppm inside the furnace and 48 ppm after dilution. This outgoing concentration is still considerably below 120 ppm, which may be a future NO_x emission limit for Stena Aluminum's smelting plant (table 4.1). In general, the results showed that an increased HCN concentration of the fuel gas led to an increasing NO formation. This increased NO concentration led to an increasing concentration of NO_2, which covers the NO formation theory for HCN, presented in section 3.3. Also the N_2O concentration was increasing with an increased NO concentration. The dilution air, introduced to cool down the temperature after the furnace, led to a considerable decrease of NO_x ($\approx$ 30 times) for all regarded fuels. Thus, the fulfillment of future NO_x limitations of 120 ppm would be possible without the installation of additional NO_x cleaning equipment, when co-firing with waste-derived fuel would be applied.
The highest HCl concentration was simulated for $WEEE_{LF}$ with 1400 ppm inside the furnace and 170 ppm after dilution. This value is 17 times higher than the HCl emission limitations of 10 ppm Stena Aluminum needs to consider today. The lowest HCl concentration after dilution was observed for Rubber (0.4 ppm), PFO (1.5 ppm), cable plastics (2.2 ppm) and $WEEE_{Inc.}$ (3.0 ppm) which all lied considerably below the limit of 10 ppm. It needs to be mentioned that the data for cable plastics were based on a dechlorinized pyrolysis gas. Therefore, a higher HCl concentrations would occur for cable plastics without this pre-treatment. Regarding the general results for the main chlorine species HCl, PUR showed slightly higher concentrations than $WEEE_{Inc.}$ even though the chlorine content (introduced as HCl) was higher for last mentioned. This was observed vice versa for Cl, wherefore it could be stated that more Cl stayed bound as HCl in the $WEEE_{Inc.}$ fuel gas. To get a better understanding of the actual impact of all regarded halogens (Cl, Br, F), which were considered as Cl in this thesis, and their potential interaction with the oxidizing inhibitor salt containing alkaline elements (Na, K), further investigations and measurements are necessary.
The results regarding SO_x emissions, showed the highest SO_2 concentration for PUR with 1400 ppm inside the furnace and 67 ppm after dilution. This concentration would exceed the SO_x emission limit of 29 ppm, which may be applied in future. All other fuels showed lower concentrations (< 15 ppm) and could fulfill this potential future limitation. For example, PFO showed a SO_2 concentration of 187 ppm inside the furnace, but decreased with dilution down to 8 ppm. Also for SO_x emissions, additional measurements and investigations need to be performed to enhance the understanding of potential interactions in an aluminum smelting process.

Besides the results of the simulations regarding NO_x, SO_x and HCl emission, also the yearly availability, the ash content, the oxygen requirement and the LHVs were part of the evaluation process. As a first step of selection, three different waste-derived fuels were selected before different sensitivity analysis were performed to cover certain process uncertainties. As a first potential fuel, PFO was selected due to its high yearly availability of 28000 tons. Also its NO_x, SO_x and Cl behavior, investigated in the simulations, showed promising results in terms of fulfillment of existing and potential future emission limitations. In addition to that, the ash content of 0.8% (0.2 g/s) for PFO showed the lowest concentration among all regarded fuel. SLF was selected as a second fuel for the sensitivity analysis, not only due to its high yearly availability of 65000 tons but also to consider the general effects on emissions of a waste-derived fuel with a comparatively high chlorine content. Furthermore, its high ash content of 45% (46 g/s) keeps the possibility of investigating the effect of solids on the aluminum smelting process, with regard to dross formation and the quality of outgoing aluminum. It should be mentioned that SLF shows variations in its LHV, as the content of organic and inorganic substances can vary a lot. These variations would lead to a fluctuating fuel requirement when co-combustion on an energy base is applied. As a third choice, $WEEE_{Inc.}$ was chosen because of its lower chlorine content compared to $WEEE_{LF}$. The general effects of highly chlorinated fuels were already covered by choosing SLF, which made an additional consideration redundant. Another selection criteria considered for $WEEE_{Inc.}$ is based on its low ash content of 5.9% (1.7 g/s) as almost no ash influence can be expected during its co-combustion.
For some fuels, their considerably higher oxygen requirement per MJ was an exclusion criteria (shown in appendix A). For example, PUR would lead to a theoretical increase in oxygen of 90% compared to the combustion of pure propane. Such an alternative fuel would lead to an increase of the running costs for oxygen, which would need to be weighed upon the propane savings resulting from their co-combustion. Not only the increased oxygen requirement but also the high ash content of 50% (53 g/s) and SO_x emissions led to an exclusion of PUR. Also its high nitrogen content (introduced as HCN) led to increased NO_x formation. Likewise, cable plastic was not considered as it showed similarities to PFO in the CHEMKIN fuel gas composition and was considered to be partly covered. However, this assumption might not be valid in reality as cable plastics are derived in a solid form and PFO in a liquid form. Besides, the availability of Cable plastics was low compared to PFO, regarding Stena Recycling International's waste stream data. In addition, no elementary analysis data were available for PUR and cable plastics, which differed for the other investigated fuels. $WEEE_{LF}$ was excluded, as its high chlorine content may cause considerable problems with respect to chlorine containing species. It was also assumed, that the effect of a high chlorine content was covered by SLF, which may not be valid in reality. Rubber was excluded, as no waste streams were measured, and its chemical behavior regarding S, N and Cl was considered to be fulfilled by the three selected fuels.
Due to a lack of available data, the model in this thesis had to be based on assumptions and simplifications, which differ from the real process. In the real smelting process, the combustion conditions vary strongly during one batch of aluminum as additional organic and inorganic compounds are introduced with the aluminum scrap but were disregarded in this work. These additional substances, together with the exothermal

aluminum oxidation process lead to dynamic temperature and stoichiometry conditions during one batch of aluminum. These dynamics have a strong influence on the resulting emissions, as strong fluctuations can be seen. In this thesis the dynamics of the batch process were disregarded and simplified to a stationary combustion environment. To cover these simplifications, different sensitivity analysis were performed regarding the oxygen availability inside the furnace, the temperature conditions and the residence the in both, the whole furnace and the high temperature flame zone. For all sensitivity analysis, general trends for selected species should be considered more than absolute numbers. The sensitivity analysis covering the oxygen availability, showed a formation peak of NO around $\lambda = 2.0$. After this, a dilution effect was visible, which could be explained as no further NO formation is possible for $\lambda > 2.0$. The HCl concentration showed a decreasing behavior with increased λ, which is a result of dilution. SO_2 peaked at $\lambda = 0.75$ and was diluted afterwards. Regarding temperature conditions observed in the sensitivity analysis, a change of the peak combustion temperature showed, that the effects of SO_x were comparatively small compared to NO_x, and that HCl formation was not affected by changing the peak temperature of combustion. Changing the average temperature inside the furnace, led to an increase in NO formation for higher average temperatures and to a decrease for low average temperatures whereas, a vice versa effect was observed for NO_2 formation. Thus, the uncertainties regarding process temperatures were covered to a large extend, without the consideration of absolute numbers. The sensitivity analysis regarding the residence time in the high temperature combustion zone has shown general trends for PFO and $WEEE_{Inc.}$ but a controversial behavior for SLF, which could be investigated in more detail in a future work. For all three fuel, a prolonged residence times in the high temperature combustion zone resulted in an increased NO concentration.
Finally, based on the selected fuels and the different eligibility criteria, PFO resulted as the appropriate co-firing fuel. This waste-derived fuel showed an overall acceptable combustion behavior regarding NO_x and SO_x emissions, which might be important for Stena Aluminum's future emission limitations. Not to mention, its yearly availability, the low ash content and its high LHV, which is in the order of propane, makes PFO the best option. In terms of the fuel feeding, PFO is appropriate due to its liquid characteristics, therefore it is comparatively easy to feed in the process. For the co-combustion of propane with PFO a number of dual-fuel burner systems for one gaseous and one liquid fuel are commercially available. This would diminish feeding expenditure, as no special feeding system (i.e. screw feeding) would be necessary. Such a dual-fuel burner system could be comparatively easy retrofitted to the existing process. Additionally, no complicated pre-treatment such as fine grinding or milling would be necessary and no extra carrier gas would be needed.

7.1. Economic evaluation

To enhance the choice of PFO as the optimum waste-derived fuel for a potential co-combustion, an economic calculation was performed. Hereby, the cost savings caused by a lower propane consumption were considered as well as potential pre-treatment costs for certain fuel alternatives. It should be mentioned that this cost were estimated without the consideration of absolute numbers. Thereby, the cost of PFO pre-treatment were estimated to be the lowest among the other alternatives, as PFO is already available in liquid form and may not need any further pre-treatment except minor steps such as sieving. Thus, only pumping cost where considered without any absolute numbers. The pre-treatment costs for SLF and $WEEE_{Inc.}$ were considered to be higher than the costs for PFO, as grinding or milling, separation and sieving would be necessary. Furthermore, a carrier gas would be needed for fuel feeding. The results of the economic calculations are summarized in a table which can be found in appendix D, where all important assumptions are included. It was found that, PFO showed the highest potential for minimizing running cost with only a slight increase in oxygen consumption of 0.8%, compared to pure propane combustion. SLF showed, due to its low LHV, the lowest potential for saving with a theoretically calculated 27% increase in oxygen requirement. $WEEE_{Inc.}$ showed a potential 4.6% decrease in oxygen consumption, but lower savings in running cost as higher expenditures for pre-treatment were assumed. Thus, PFO was concluded to be the optimum co-firing option in an economical point of view, as the highest savings in the running costs can be expected. Besides, a retrofit would be less complicated as dual-fuel systems for gaseous and liquid fuels are available and do not demand complicated feeding equipment.

8. Conclusions

Co-combustion simulations for seven different waste-derived fuels with propane for Stena Aluminum's recycling facility located in Älmhult, Sweden have shown major advantages for process fuel oil (PFO). Regarding the theoretical combustion behavior resulted from CHEMKIN PRO simulations, PFO has shown no major increases of SO_x, NO_x and chlorine release, whereas other fuel alternatives like WEEE(Landfill) and PUR had to be excluded due to very high HCl, SO_2 and SO_3 content. Thereby, PFO was not the only fuel showing good co-combustion characteristics in the simulations, but regarding its yearly availability and its naturally liquid aggregate phase it was concluded to be the optimum fuel for co-firing in the regarded aluminum smelting process. Also an economic calculation showed the highest saving potential for PFO regarding running cost. Furthermore, several co-combustion burners are commercially available which can be applied with gaseous and liquid fuels. Thus, a retrofit of the existing smelting system would be comparatively easy to adapt and therefore economically attractive. Besides, the very high heating value of PFO (which lies in the order of propane), its very low ash content and its oxygen requirement per MJ might not cause major changes in today's overall fuel and oxygen consumption and may not affect the quality of the outgoing aluminum. Thus, process changes would not affect the aluminum smelting process and its throughput, which would lead to the possibility of economic savings by a reduction in fuel costs. However, it needs to be emphasized that the combustion conditions during the smelting process of aluminum vary strongly with regard to temperatures and the oxygen availability which both has a strong effect on the pollutant formation. Therefore, the outgoing concentration of pollutants may fluctuate considerable during one batch which needs to be considered in reality, especially with regard to potential future emission limitations. Additionally, the CHEMKIN results are based on a gas phase simulation even though the investigated waste-derived fuels are either solid or liquid, which may lead to overall differences regarding pollutant formation.

9. Future work

In a short term perspective, investigations with focus on the organic and inorganic compounds entering the process together with the aluminum need to be done. Therefore, measurement campaigns especially regarding NO_x, SO_x and particle emissions need to be applied for a number of different batches. In this context, it might also be helpful to investigate potential future emission limitations with a particular respect to the co-combustion of waste-derived fuels in an aluminum recycling plant. Additionally, an optimization of process running conditions with focus on emission minimization could be assessed, in which strong fluctuations of emissions during one batch may be minimized. In a long term perspective, co-combustion might become an interesting option not only for secondary aluminum smelting facilities but also for other energy intensive industries, regarding the economic saving potential. Therefore, more research needs to be done with focus on pollutant formation and potential process changes induced by co-firing. Especially, highly chlorinated and brominated fuels need to be investigated in more detail, as a very high chlorine and bromine content might lead to major changes in the ongoing combustion chemistry. Regarding aluminum recycling, the effect of aluminum oxide formation needs to be investigated in more detail as this might affect the overall temperature conditions inside the furnace. Therefore, CFD simulations need to be done, considering the ongoing reactions and processes inside the smelting furnace in more detail (i.e. also mechanical rotation, tilting and its effect on the combustion process). Also the inhibitor salt added to the process with the purpose of dross formation could be considered in a future work, as the salt contains K and Na, which have a well known effect on the combustion chemistry. However, the evaluation of this effect has not been researched in reality yet. In addition to a research specified on aluminum recycling processes, the co-combustion of PFO could be investigated in further detail, as this fuel does not only show a very high abundance, but also a high LHV and comparatively low emissions. Thereby, different feeding technologies and burner systems could be analyzed in more detail in order to find an optimum solution for the fuel feeding and its co-combustion.

Bibliography

[1] M. E. Schlesinger, (**2002**).
Title: Aluminum Recycling
Publisher: CRC Press, University of Missouri-Rolla, Rolla, MO, USA.
ISBN: 978-0-8493-9662-5

[2] A.R. Khoei, I. Masters, D.T. Gethin, (May **2002**).
Title: Design optimization of aluminum recycling processes using Taguchi technique
Publisher: Published by Elsevier Science B.V.
Journal: of Materials Processing Technology 127, 96-106
PII: S0924-0136(02)00273-X

[3] International Aluminum Institute,(**2009**).
Title: Global Aluminium Recycling: A Cornerstone of Sustainable Development, p. 28
Institute: International Aluminum Institute
URL: www.world-aluminium.org/media/filer_public/2013/01/15/fl0000181.pdf

[4] Organization of European aluminum refiners and remelters (OEA) (**2015**).
Title: Recycling aluminum: A pathway to an sustainable economy
URL: www.european-aluminium.eu/wp-content/uploads/2011/08/Recycling-Aluminium-2015.pdf

[5] J. Morrison, (**2005**).
Title: European aluminium recycling under threat?
Journal: Alum. Int. Today, **17**(1), 17

[6] R.J. Anderson, (**1931**).
Title: Secondary Aluminum
Booklet: Sherwood Press, Cleveland, OH,

[7] K.J., Martchek, (**1997**).
Title: Life cycle benefits, challenges, and the potential of recycled aluminum, in Process Air and Waste Manage.
Paper: Paper 97-RP124B.01

[8] J. van Linden, (**1990**).

Title: Aluminum recycling: everybody's business, technological challenges and opportunities, in Light Metals.
Paper: Bickert, TMS-AIME, Warrendale, PA, p. 675.

[9] K. Veijonen et al.,(**2003**-03).
Title: Biomass co-firing - an efficient way to reduce green house gas emissions
Publisher: EUBIONET - European Bioenergy Networks
URL: ec.europa.eu/energy/sites/ener/files/documents/ 2003_cofiring_eu_bionet.pdf

[10] P. Lempp et al.,(**2013**-01).
Title: Biomass Co-firing
Publisher: International Energy Agency - Energy Technology Systems Analysis Programme (IEA-ETSAP)
URL: www.irena.org/DocumentDownloads/Publications/ IRENA-ETSAP%20Tech%20Brief%20E21%20Biomass%20Co-firing.pdf

[11] J. Blomberg, S. Hellmer,(**1999**).
Title: The economics of the west European secondary aluminium industry, a short-run equilibrium model approach, 35-47
Conference: Proceedings of the Fourth ASM International Conference and Exhibition on the Recycling of Metals
Address: Vienna, Austria

[12] Organization of European aluminum refiners and remelters (OEA) (**2007**).
Title: Aluminium Recycling in Europe: The Road to High Quality Products
URL: www.european-aluminium.eu/wp-content/uploads/2011/08/ Aluminium-recycling-in-Europe-2007.pdf

[13] D. Drohmann, L. Tange,(**2004**).
Title: The implementation of the WEEE-directive: An opportunity for plastics containing brominated flame retardants?
Journal: Flame Retardants, **11**, Interscience

[14] Ranch Cryogenics, Inc.,(**2016**).
Title: Basic Air Separation Unit Description
Publisher: Ranch Cryogenics, Inc.
URL: www.ranchcryogenics.com/about/basic-air-separation-unit- description/ [2016-02-13]

[15] C. E. Baukal,(**2003**).
Title: Industrial Burners Handbook, chap. 11-22
Publisher: CRC Press
ISBN: 0-8493-1386-4

[16] R.J. Reed,(**1995**).
Title: North American Combustion Handbook, Vol.2
Publisher: The North American Manufacturing Company
ISBN: 978-0960-1596-11

[17] P. Basu, C. Kefa, L. Jestin,(**2000**).
Title: Boilers and Burners
Publisher: Springer
ISBN: 978-1-4612-7061-4

[18] J.N. Newby,(**1985**).
Title: The Regenerative Burner: Principles, Properties and Practice, in Industrial Heat Exchangers, p. 77-80
Publisher: American Society of Metals, Warren, PA
ISBN: 978-1-4398-4213-3

[19] I. Nakamachi et.al.,(**1996**-11-05).
Assignee: Regenerative Burner, Burner System and Method of Burning
Title: Ultra-low NOx burner assembly
Patent-No.: US 5571006

[20] H. Kobayashi, L.E. Bool,(**2005**-10-25).
Assignee: Praxair Technology, Inc.
Title: Oxygen enhanced low NOx combustion
Patent-No.: US 6957955 B2

[21] T. Wechsler, G. Gitman, (**1990**).
Title: Use of the Pyretron variable ratio air/oxygen/fuel burner system for aluminum melting, p. 269
Workshop: Energy Conservation Workshop XI: Energy and the Environment in the 1990s
Publisher: Aluminum Association, Washington DC

[22] R.M. McGuinness, W.T. Keinberg,(**1998**).
Title: Oxygen Production, Chapter 3 in Oxygen-Enhanced Combustion
Publisher: CRC Press, Boca Raton, (FL)

[23] L. Gluns, S. Schemberg,(**2003**).
Title: Advantages of oxy-fuel burner systems for aluminum recycling
Booklet: Aluminium World: Product design and applications
Company: Air Products PLC, UK
URL: www.airproducts.com/-/media/Files/PDF/industries/metals-advantages-oxy-fuel-burner-systems-aluminium-recycling.pdf

[24] J. Cao, A. G. Slavejkov,(**2007**-11-01).
Assignee: Air Products And Chemicals, Inc.
Title: Ultra-low NOx burner assembly
Patent-No.: US 8696348

[25] R. Hewertson,(**2005**).
Title: When does oxy-fuel make sense?
URL: www.c2es.org/docUploads/Air%20Products%20-%20When%20does%20oxy%20fuel%20make%20sense.pdf

[26] The engineering tool box,(**2016**).
Title: The engineering tool box
URL: http://www.engineeringtoolbox.com/flame-temperatures -gases-d_422.html

[27] T. Kudra, A.S. Mujumdar,(**2002**).
Title: Advanced Drying Technologies
Publisher: CRC Press
ISBN: 978-1420-0738-74

[28] T. Davies,(**1986**).
Title: Regenerative burners for radiant tubes field test experience, in Industrial Combustion Technologies, 77-85
Publisher: American Society of Metals

[29] D. Venizelos,W. Bussman, R. Hayes, R. Poe,(**2001**).
Assignee: T. Venizelos Demetris
Title: High Capacity/Low NOx Radiant Wall Burner
Patent-No.: US 20020076668 A1

[30] S. Dick,(**1996**-08-13).
Assignee: L'Air Liquide, Societe Anonyme Pour L'Etudeet L'Exploitation Des Procedes Georges Claude, Paris
Title: ASYMMETRIC OXYGEN/FUEL BURNER
Patent-No.: US 5545033

[31] L.T. Yap,(**1995**-10-03).
Assignee: The BOC Group, Inc.
Title: AIR-OXY-FUEL BURNER METHOD AND APPARATUS
Patent-No.: US 5454712

[32] D.M. Gross,(**2003**-07-22).
Assignee: Jupiter Oxygen Corporation, Schiller Park (IL)
Title: METHOD FOR OXY-FUELED COMBUSTION
Patent-No.: US 6596220 B2

[33] D.M. Gross,(**2002**-08-20).
Assignee: Jupiter Oxygen Corporation, Schiller Park (IL)
Title: OXY-FUEL COMBUSTION SYSTEM AND USES THEREFOR
Patent-No.: US 6436337 B1

[34] B. Courtemanche,(**2012**).
Title: Dual Fuel Firing: The New Future for the Aging U.S. Based Coal-Fired Boilers
Publisher: Babcock Power Inc.
URL: www.babcockpower.com/pdf/RPI-TP-0228.pdf

[35] U.S. Department of Energy,(**2000**).
Title: Biomass co-firing: A renewable alternative for utilities
Publisher: U.S. Department of Energy
URL: www.nrel.gov/docs/fy00osti/28009.pdf

[36] S. Wilcox,(**2010**-04-13).
Title: Monitoring Co-firing and Oxycoal Burners using Optical Sensors
Publisher: University of Prifysgol
URL: www.coalresearchforum.org/crfagm2013/S%20Wilcox, %20Glamorgan, %20Cranfield,%2010-04-13.pdf

[37] M.T. Nguyen et al.,(**2016**).
Title: Release of chlorinated, brominated and mixed halogenated dioxin-related compounds to soils from open burning of e-waste in Agbogbloshie (Accra, Ghana)
Journal: Journal of Hazardous Materials, **302**, p. 151 - 157

[38] R. Cossu, T. Lai,(**2016**).
Title: Automotive shredder residue (ASR) management: An overview
Journal: Waste Management, **45**, p. 143 - 151

[39] Nuria Ortuño et al.,(**2014**-11-15).
Title: Pollutant emissions during pyrolysis and combustion of waste printed circuit boards, before and after metal removal
Journal: Science of The Total Environment, **499**, p. 27 - 35

[40] D. Bankiewicz et al.,(**2016**).
Title: High temperature corrosion of boiler waterwalls induced by chlorides and bromides - Part 2: Lab-scale corrosion tests and thermodynamic equilibrium modeling of ash and gaseous species
Journal: Fuel, **94**, p. 240 - 350

[41] S. Gao et al.,(**2016**).

Title: Desulfurization of fuel oils: Mutual solubility of ionic liquids and fuel oil
Journal: Fuel **173**, p. 164 - 171

[42] A. Pawelec et al.,(**2016**).
Title: Pilot plant for electron beam treatment of flue gases from heavy fuel oil fired boiler
Journal: Fuel Processing Technology **145**, p. 123 - 129

[43] X. Wei et al.,(**2004**).
Title: Interactions of CO, HCl, and SO_x in pulverised coal flames
Journal: Fuel **83**, p. 1227 - 1233

[44] Brusselers, J., D.F.E. Mark, and L. Tange, (**2006**).
Title: USING METAL-RICH WEEE PLASTICS AS FEEDSTOCK / FUEL SUBSTITUTE FOR AN INTEGRATED METALS SMELTER
Publisher: Plastics Europe in cooperation with Umicore and EFRA, p. 20.

[45] I. Vermeulen et al.,(**2011**).
Title: Automotive shredder residue (ASR): Reviewing its production from end-of-life vehicles (ELVs) and its recycling, energy or chemicals' valorisation
Journal: Journal of Hazardous Materials, **190**, p. 8 - 27

[46] M. Takeda et al.,(**2005**).
Title: Fate of the chlorine and fluorine in a sub-bituminous coal during pyrolysis and gasification
Journal: Fuel, **85**, p. 235 - 242

[47] P. Glarborg,(**2007**).
Title:Hidden interactions-Trace species govering combustion and emissions
Journal: Proceedings of the Combustion Institute, **31 I**, p. 77 - 98

[48] C.F. Cullis, M.F.R. Mulcahy,(**1972**).
Title: The kinetics of combustion of gaseous sulfur compounds
Journal: Combustion and Flame, **18**(2), p. 225 - 292

[49] E. Krawczyk et al.,(**2013**).
Title: The chemical mechanism of SOx formation and elimination in coal combustion process
Journal: CHEMIK, (**67**)-10, 856?862

[50] D. Lindberg, R. Backman, P. Chartrand(**2006**).
Title: Thermodynamic evaluation and optimization of the (Na_2SO_4 + K_2SO_4 + $Na_2S_2O_7$ + $K_2S_2O_7$) system
Journal: Journal of Chemical Thermodynamics, **38**(12), p. 1568 - 1583

[51] L. Deng, X. Jin, Y. Zhang, D. Che,(**2016**).
Title: Release of nitrogen oxides during combustion of model coals
Journal: Fuel, **175** p. 217 - 224

[52] C. Zhu et al.,(**2015**).
Title: NOx emission characteristics of fluidized bed combustion in atmospheres rich in oxygen and water vapor for high-nitrogen fuel
Journal: Fuel, **139** p. 346 - 355

[53] M.R. Beychok,(**1973**-03).
Title: NOX emission from fuel combustion controlled
Journal: The Oil and Gas Journal, p. 53 - 56

[54] Y.B. Zeldovich,(**1946**).
Title: The Oxidation of Nitrogen in Combustion Explosions
Journal: Acta Physicochimica U.S.S.R. **21**, p. 577 - 628

[55] G.A. Lavoie et al.,(**1970**).
Title: Experimental and Theoretical Study of Nitric Oxide Formation in Internal Combustion Engines
Journal: Combustion Science Technology **4**, p. 313 - 326

[56] R. Edland, F. Normann, K. Andersson,(**2014**).
Title: Nitrogen chemistry in rotary kiln flames: Impact of mixing rate and temperature at high air to fuel ratios
Publisher: Chalmers University of Technology, Division of Energy Technology, Department of Energy and Environment

[57] V. Kermes,(**2008**).
Title: Testing of gas and liquid fuel burners for power and process industries
Journal: Energy, **33** p. 1551 - 1561

[58] P. Sun et al.,(**2013**-04).
Title: Experimental investigation on the combustion and heat transfer characteristics of wide size biomass co-firing in 0.2 MW circulating fluidized bed
Journal: Applied Thermal Engineering **52**(2) p. 284 - 292

[59] C.L. Brooks,(**1970**).
Title: Basic Principles of Aluminum Melting, Metal Preparation, and Molten Metal Handling, p. 55
Publisher: Reynolds Metals Co., Richmond (VA)

[60] J.P. McKenna, A. Wisdom,(**1997**).
Title: Die Casting Engineer, 41(**6**), p. 64

Publisher: CRC Press

[61] D.E. Groteke, J. Fieber,(**1999**).
Title: A melt performance comparison: stack melter vs. reverberatory furnace
Publisher: Modern Casting, 89(**3**), 50

[62] E. Kear, et al.,(**2000**).
Title: An innovative stack melter for use in the aluminum casting industry, p. 901
Symposium: 2nd International Symposium of recycling metals

[63] LAC group.
Title: Melting and holding electric resistance stationary furnaces PT Mk.II
URL: http://www.lac.cz/en/produkty/katalogove-pece-susarny/prumyslove-pece-slevarny/melting-and-holding-electric-resistance-stationary-furnaces-/?gclid=CKeA1LXq98wCFSH3cgodxrcJsA

[64] HERTWICH SMS group,(**2011**).
Title: Single Chamber Melting and Casting Furnace
URL: http://www.hertwich.com/index.php?id=melting_furnaces

[65] HERTWICH SMS group,(**2011**).
Title: Multi Chamber Furnace (type Ecomelt)
URL: http://www.hertwich.com/index.php?id=casting_furnaces

[66] C.J. Schmitz (Author),(**2007**).
Title: Handbook of Aluminium Recycling, p.110-120
Publisher: Vulkan-Verlag GmbH
ISBN: 978-3802-7293-62

[67] HERTWICH SMS group,(**2011**).
Title: Universal Rotary Tilting Furnace (URTF)
URL: www.hertwich.com/index.php?id=148

[68] Insertec,(**2016**).
Title: FARB Tilting Rotary Furnace
URL: http://www.insertec.biz/en/industrial-furnaces/aluminium-recycling-furnaces/rotary-furnace

[69] Indotherm equipment corporation,(**2011**).
Title: Rotary Melting Furnace
URL: http://www.indotherms.com

[70] B. Friedrich,(**2001**).

Title: Improved Aluminium Recovery at Recycling Plants by integrated Slag Refining
URL: http://www.metallurgie.rwth-aachen.de/old/images/pages/publikationen/improved_alumin_id_8157.pdf

[71] C. Paitoni, L. Benedini,(**2004**).
Title: Rotary smelting furnace
Journal: Diecasting technology

[72] C. Hall,(**2004**).
Title: Turn and tilt to melt mixed aluminium scrap

[73] U.M.J. Boin, M.A. Reuter, Th. Probst,(**2004**).
Title: Measuring - Modelling: Understanding the Al Scrap Melting Processes inside a Rotary Furnace
Journal: World of metallurgy, ERZMETALL, **57**, p. 266 - 271

[74] V. Salet,(**2003**).
Title: Steady State Mass and Energy Balance Model of the Rotary Furnace: Study to Determine the Burn-off Rate of Aluminium Metal inside a Rotary Furnace
Thesis: M.Sc. Thesis, Department of Applied Earth Sciences, Delft University of Technology

[75] R.D., Peterson,(**1990**).
Title: Effect of salt flux additives on aluminum droplet coalescence
Symposium: 2nd International Symposium of recycling metals

[76] PE Americas,(**2010**-05-21).
Title: Life Cycle Impact Assessment of Aluminum Beverage Cans, p.70-85
Publisher:Aluminum Association, Inc. Washington, D.C.
URL: www.container-recycling.org/assets/pdfs/aluminum/LCA-2010-AluminumAssoc.pdf

[77] STENA METALL AB,(**2016**-02-16).
Title: In cooperation with STENA METALL AB

[78] European Environment Agency,(**2010**-10-15).
Title: Nitrogen oxides (NOx) emissions
URL: http://www.eea.europa.eu/data-and-maps/indicators/eea-32-nitrogen-oxides-nox-emissions-1

[79] Bundesministerium für Umwelt, Naturschutz und Reaktorsicherheit,(**2002**-07-24).
Title: TA Luft - Erste Allgemeine Verwaltungsvorschrift zum Bundes -Immissionsschutzgesetz

URL: www.bmu.de/files/taluft.pdf

[80] EUROPEAN PARLIAMENT,(**2015**-11-25).
Title: DIRECTIVE (EU) 2015/2193 OF THE EUROPEAN PARLIAMENT AND OF THE COUNCIL
URL: http://eur-lex.europa.eu/legal-content/EN/TXT/?uri=CELEX:32015L2193

[81] J.M. Johansen et al.,(**2011**).
Title: Release of K, Cl, and S during combustion and co-combustion of high-chlorine biomass
Journal: Energy and Fuels, **25**(11), p. 4961 - 4971

[82] STENA Metall R& D,(**2016**).
Title: Internal data provided by STENA Metall
Congress: Plastic Chemical Recovery for Production of Chemical Intermediates at a Swedish Chemical Cluster (PECREST), 2016-03-04

[83] A. Sepúlveda et al.,(**2010**).
Title: A review of the environmental fate and effects of hazardous substances released from electrical and electronic equipments during recycling: Examples from China and India
Journal: Environmental Impact Assessment Review, **30**, p. 28 - 41

[84] A. Holleman, E. Wiberg ,(**2001**).
Title: Inorganic Chemistry
ISBN: 0-12-352651-5

[85] P.Glarborg, M.U. Alzueta, K. Dam-Johansen, J. A. Miller,(**1998**).
Title: Kinetic Modeling of Hydrocarbon/Nitric Oxide Interactions in a Flow Reactor
Journal: Combustion Flame, **105** p. 1 - 27

[86] L. Hindiyarti et al.,(**2008**).
Title: An exploratory study of alkali sulfate aerosol formation during biomass combustion
Journal: Fuel, **87**(8-9), p. 1591 - 1600

[87] H. Kassmann et al.,(**2013**).
Title: Two strategies to reduce gaseous KCl and chlorine in deposits during biomass combustion - Injection of ammonim sulphate and co-combustion with peat
Journal: Fuel processing technologies, (**105**), p. 170 - 180

[88] B. Olanders, B.M. Steenari,(**1995**).
Title: Characterization of ashes from wood and straw
Journal: Biomass and Bioenergy, **8**(2), p. 105 - 115

[89] M. Slack et al.,(**1989**).
Title: Potassium kinetics in heavily seeded atmospheric pressure laminar methane flames
Journal: Fuel, **77**(3-4), p. 311 - 320

[90] P. Dagaut, P. Glarborg, M.U. Alzueta,(**2008**).
Title: The oxidation of hydrogen cynide and related chemistry
Journal: Prog. Energy Combustion Science, **34**, p. 1 - 46

[91] O. Skreiberg,P. Kilpinen, P. Glarborg,(**2004**).
Title: Ammonia Chemistry under fuel-rich conditions in a flow reactor
Journal: Combustion Flame, **136** p. 501 - 508

[92] C.L. Rasmussen, P.Glarborg,(**2008**).
Title: Sensitizing Effects of NO_x on CH_4 Oxidation at High Pressure
Journal: Combustion Flame

[93] P.Glarborg, A.B. Bendtsen, J. A. Miller,(**1999**).
Title: Nitromethane Dissociation. Implications for the CH_3 + NO_2 Reaction
Journal: International Journal of Chemistry Kinetics, **31** p. 591 - 602

[94] B. Zhou, Y. Yang, M.A. Reuter, U.M.J. Boin,(**2005**).
Title: CFD BASED PROCESS MODELLING OF A ROTARY FURNACE FOR ALUMINIUM SCRAP MELTING
Journal: Delft University of Technology, Department of Applied Earth Sciences, Mijnbouwstraat 120, 2628 RX Delft, The Netherlands

[95] S. Murza, B. Henning, H.D. Jasper,(**2007**-02).
Title: CFD-simulation of melting furnaces for secondary aluminum
Publisher: HEAT PROCESSING, Vulkan-Verlag GmbH

[96] A.R. Khoei, I. Masters, D.T. Gethin,(**2003**).
Title: Numerical modelling of the rotary furnace in aluminium recycling processes
Journal: Journal of Materials Processing Technology **139** p. 567 - 572

[97] Buitrago, P.A., et al., (**2013**).
Title: Impinger-based mercury specification methods and gas-phase mercury oxidation by bromine in combustion systems
Journal: Energy and Fuels, **27**(10): p. 6255-6261.

[98] Van Otten, B., et al., (**2011**).
Title: Gas-phase oxidation of mercury by bromine and chlorine in flue gas.
Journal: Energy and Fuels, **25**(8): p. 3530-3536.

[99] Rademakers, P.H., W., van de Wetering, J., (**2002**).
Title: Review on corrosion in waste incinerators and possible effect of bromine.
Publisher: TNO Industrial Technology Apeldoorn, Netherlands.

[100] Vainikka, P., et al., (**2011**).
Title: Bromine as an ash forming element in a fluidized bed boiler combusting solid recovered fuel.
Journal: Fuel, **90**(3) p. 1101-1112.

[101] E. Kantarelis, P. Donaj, W.Yang, A. Zabaniotou, (2009)
Title: Sustainable valorization of plastic wastes for energy with environmental safety via High Temperature Pyrolysis (HTP) and High-Temperature Steam Gasification (HTSG)
Journal: Journal of Hazardous Materials
Publisher: Elsevier B.V.

[102] P. Donaj et al., (2010)
Title: Recycling of automobile shredder residue with a microwave pyrolysis combined with high temperature steam gasification
Journal: Journal of Hazardous Materials
Publisher: Elsevier B.V.

[103] Cooperation with Stena, (2015)
Title: Analysis of KEO

[104] Cooperation with Stena Technoworld, (2015)
Title: Analysis of WEEE (incinartion)

[105] Cooperation with Stena Technoworld, (2015)
Title: Analysis of WEEE (landfill)

[106] Cooperation with STENA Metall, (2012)
Title: Survey of thermo-chemical treatment of SLF

Appendix A.

Appendix: Potential alternative fuels for aluminum recycling

This chapter should provide a overview of the alternative fuels regarded in this work. Thereby an elemental chemical analysis of each potential contributor is presented. It should be mentioned that the pre-processing for fuel production (pyrolysis, gasification) is not going to be discussed any deeper in this work. Thus only chemicals elements remaining in an usable fuel will be listed here. Additionally, the elementary fuel analysis only considers the fractional elementary content of the investigated probe and may not be overall representative. Therefore, the chemical composition may vary considerably between different waste sources dependent on the initial product, which also results in changing emission conditions as well as different heating values.

Elementary analysis of alternative fuel:

Cable plastics:

Produced as granulates (2-8 mm) from electric cable recycling, contain mainly XLPE. XLPE cable plastics contains no heavy metals, but some Al. Cl-content is < 0,1 %. PVC cable plastics contain inorganic fillers ($CaCO_3$), the Cl-content is high about 20 %. HFFR cable plastics contain organic fillers ($Al(OH)_3$, $Mg(OH)_2$) up to 60 % w/w. The elementary fuel analysis is shown in following table. It should be mentioned that the composition of cable plastics is based on a pyrolyzed gas, which has been dechlorinated before the pyrolysis.

Combustible gas composition of cable plastics

Elements	**dry [wt %]**	**weighted [wt %]**
C	67.640	68.247
H	9.480	9.565
S	0.001	0.001
N	0.070	0.071
Cl	0.170[a]	0.172
O	21.750	21.945
F	0.000	0.000
Br	0.000	0.000
SUM:	**99.111**	**100.000**
Thermal value		
Heating value [MJ/kg]	32.0	
Moisture content		
Moisture [% g_{H_2O}/g_{Total}]	0.24	
Ash content		
Ash content [dry %]	13.98	

Source: [101]

[a] The fuel has been dechlorinized before the pyrolysis.

Polyurethane (PUR):

Polyurethane produced from recycling of freezers and coolers. Contain nitrogen and oxygen as a part of the polymer. Is today used as an oil-absorbent and sent for incineration. Maximum 0.1 % Cl, the fragmentation removes residual CFC-based blowing agents. The elementary fuel analysis is shown in following table. It should be mentioned that the composition PUR is based on a pyrolyzed gas, which has been dechlorinated before the pyrolysis.

Combustible gas composition of PUR

Elements	**dry [wt %]**	**Weighted [wt %]**
C	38.760	77.847
H	2.670	5.363
S	1.180	2.270
N	3.580	7.190
Cl	0.600[a]	1.205
O	3.000	6.025
F	0.000	0.000
Br	0.000	0.000
SUM:	**49.790**	**100.000**
Thermal value		
Heating value [MJ/kg]	14.98	
Moisture content		
Moisture [% g_{H_2O}/g_{Total}]	2.34	
Ash content		
Ash content [dry %]	49.74	

Source: [102]

[a]The fuel has been dechlorinized before the pyrolysis.

Processed fuel oil (PFO):

A processed fuel oil (PFO) is made from oil wastes. The waste oil is treated to remove solvents and water and larger particulates. The PFO is today combusted in facilities that have permits for waste treatment (cement and waste incineration plants). This is the only fraction in the list which today has positive commercial value. The elementary fuel analysis is shown in upcoming table.

Combustible gas composition of PFO

Elements	**dry [wt %]**	**Weighted [wt %]**
C	83.54	86.094
H	12.50	12.880
S	0.731	0.753
N	0.114	0.117
Cl	0.150	0.155
O	0.000	0.000
F	0.000	0.000
Br	0.000	0.000
SUM:	**97.03**	**100.000**
Thermal value		
Heating value [MJ/kg]	41.4	
Moisture content		
Moisture [% g_{H_2O}/g_{Total}]	0.41	
Ash content		
Ash content [dry %]	0.784	

Source: [103]

WEEE (Incineration):

Electronic waste plastics mostly. Contain around 1.5 % Br and 6 % ash. Contain some metals (Fe, Al, Cu). Today sent for incineration. The elementary fuel analysis is shown in following table.

Combustible gas composition of WEEE (incineration)

Elements	**dry [wt %]**	**Weighted [wt %]**
C	72.200	75,200
H	6.300	6,562
S	0.020	0,021
N	1.600	1,666
Cl	0.240	0,250
O	14.000	14,582
F	0.150	0,156
Br	1.500	1,562
SUM:	**96,010**	**100.000**
Thermal value		
Heating value [MJ/kg]$\|_p$	30.1	
Calorific value [MJ/kg]$\|_v$	31.4	
Moisture content		
Moisture [% g_{H_2O}/g_{Total}]	12.4	
Ash content		
Ash content [dry %]	5.9	

Source: [104]

WEEE (Landfill):

Electronic waste plastics mostly (Heavy plastics). Contain around 6 % Cl and 24 % ash. Contain some metals (Fe, Al, Cu). Today put on landfills. The elementary fuel analysis is shown in following table.

Combustible gas composition of WEEE (landfill)

Elements	**dry [wt %]**	**Weighted [wt %]**
C	49.500	64,546
H	5.400	7,041
S	0.110	0,143
N	2.200	2,869
Cl	6.700	8,736
O	12.000	15,647
F	0.008	0,104
Br	0.700	0,913
SUM:	**76.690**	**100.000**
Thermal value		
Heating value [MJ/kg]$\|_p$	20.3	
Calorific value [MJ/kg]$\|_v$	21.5	
Moisture content		
Moisture [% g_{H_2O}/g_{Total}]	3.4	
Ash content		
Ash content [dry %]	24.3	

Source: [105]

Shredded light fragments (SLF):

Highly heterogeneous shredder residues from automotive and metal scrap, which have an ash fraction of 40 %. Containing plastics, wood, textiles, leather, metals, glass and rocks. The elementary fuel analysis is shown in following table.

Combustible gas composition of SLF (dry, ash free basis)

Elements	**dry [wt %]**	**Weighted [wt %]**
C	63.800	63,864
H	8,000	8,008
S	0.500	0,501
N	1.700	1,702
Cl	2.100	2,102
O	23.700	23,724
F	0.100	0,100
Br	0.000	0,000
SUM:	**99.90**	**100.000**
Thermal value		
Heating value [MJ/kg fuel]	14.3	
Calorific value [MJ/kg fuel]	15.4	
Moisture content		
Moisture [% g_{H_2O}/g_{Total}]	11.3	
Ash content		
Ash content [dry %]	44.9	

Source: [106]

Rubber:

Fraction that is going to be produced in Halmstad which includes mostly rubber and some plastics. Is regarded as a problematic fraction. There are preliminary composition estimates and the possible volumes will be announce later. The elementary fuel analysis is shown in following table.

Combustible gas composition of Rubber

Elements	**dry [wt %]**	**Weighted [wt %]**
C	84.580	93,058
H	2.820	3,103
S	1.010	1,111
N	0.120	0,132
Cl	0.030	0,033
O	2.330	2,564
F	0.000	0.000
Br	0.000	0.000
SUM:	**90.890**	**100.000**
Thermal value		
Heating value [MJ/kg]	32.12	
Moisture content		
Moisture [% g_{H_2O}/g_{Total}]	0.8	
Ash content		
Ash content [dry %]	9.11	

Source: [102]

Fractions possible as fuels within STENA Metall to replace propane

Following table shows different waste flows in Sweden in tons per year. This waste sources could possibly replace a share of propane in STENA's aluminum smelting process in Älmhult. It should be mentioned that SLF with 65000 tons/year and PFO with 28000 tons/year would be considerable choices for a propane alternative regarding an availability point of view. Also WEEE (fuel) and WEEE (landfill) with both 5000 tons per year would be considerable options among the other fuels.

Fractions possible as fuels within STENA Metall to replace propane

Fraction	**Availability [tons in Sweden/yr]**	**Feeding**
XLPE cable plastics	2500	Pulverized solid
PVC/HFFR cable plastics	3500	Pulverized solid
PUR	2500	Pulverized solid
PFO (ERC-14)	28000	Liquid
WEEE (fuel)	5000	Solid/Syngas
WEEE (landfill)	5000	Syngas
SLF	65000	Syngas
Rubber	(TBA)	Syngas

Appendix B.

Appendix: Transformation of alternative fuel into fuel gas

Using the weighted share of each element x for each alternative fuel included in the elementary analysis shown in appendix A, a respective share in $n_x = {}^{mole_x}/_{g_{fuel}}$ can be calculated. Furthermore, it is assumed that the hydrogen (H) contained in the fuel hydrogenizes primarily all S to H_2S, all N to HCN and all Cl (+ Br,+ F) to HCl. The remaining hydrogen (called secondary H) is injected as H2. Additionally all oxygen contained in the fuel is used to oxidize all C, which is not needed to form HCN, to CO. The lacking oxygen, which needs to be added to convert the fuel into a CHEMKIN fuel gas is also calculated. For the CHEMKIN PRO input, the individual molar shares n_x are weighted with the total molar weight $n_{total} = \sum n_x$. The moisture content for each fuel as been converted from a total mass base to a fuel gas mass base. All considered equations are summarized in the following shaded box.

Secondary hydrogen share introduced as H_2:

$$n_{H_2,sec} = \frac{n_H - n_{HCN} - n_{HCl}}{2} - n_{H_2S} \tag{B.1a}$$

Secondary carbon share, remaining after HCN formation:

$$n_{C,sec} = n_C - n_{HCN} \tag{B.1b}$$

Oxygen share required to oxidize all C to CO (subtracted later from the oxidizer):

$$n_{O_2,sec} = \frac{n_O - n_{CO}}{2} \tag{B.1c}$$

Total molar weight:

$$n_{Total} = \sum (n_{CO} + n_{H_2S} + n_{HCN} + n_{HCl} + n_{H_2,sec} + n_{H_2O}) \tag{B.1d}$$

Resulting CHEMKIN PRO weighted fractions in ${}^{g_x}/_{g_{Total}}$:

$$m_{weighted} = \frac{m_x}{m_{Total}} \tag{B.1e}$$

Appendix C.

Appendix: Evaluation of a reference case

For the co-firing simulations, a reference case has been selected. The selected reference case considers higher temperature conditions as well as a higher air availability inside the furnace. Thereby, the average temperate has been chosen to be 950 °C inside the furnace, which is a higher average temperature compared to CFD simulations by B. Zhou et al. [94] but lower compared to the considered average temperature of 1100 °C chosen in Stena Metall's report "Calculation of gas flow and pressure drop around the rotary kiln furnace Älmhult" from 2011-05-13 by Björn Hall. The outgoing CO_2 concentration (at 15'000 mm) is almost equal for all alternatives, since primary and secondary dilution air cause a rapid decrease of the CO_2 concentration down to around 1.5 %, which corresponds well with the measurement data provided by Stena Aluminum measured directly after the furnace. Thus, the dilutional effects considered in the simulations can be assumed to represent Stena Aluminum's process to a valuable extent. Furthermore, the reference case considers higher air availability inside the furnace (leakage air) but substoichiometric conditions regarding pure oxygen feeding, which corresponds well with Stena Aluminum's process conditions. Furthermore, the overall stoichiometry inside the furnace is kept constant at $\lambda_{\text{Furnace}} = 0.9$ for all co-firing simulations. Therefore, the oxygen profiles had to be adapted for each alternative fuel, since different oxygen requirements per MJ lead to differing behaviors compared to a pure propane combustion. For all fuel alternatives, the co-firing simulations were made regarding a power of 2 MW for the burner, fired by **60 % of propane** and **40 % of alternative fuel** on an energy basis (regarding LHVs).

Available measurement data from Stena Aluminum

For a later comparison of process conditions, when co-combusting with different alternative fuels is considered, some known measurement data from Stena Aluminum's process need to be considered. Since process emissions have changed with every new load of aluminum scrap, it is difficult to get valid average emission data. Therefore, a long term measurement campaign needs to be applied in the future. However, some measured data are considered from three different events, where only average values of each event has been selected. The measured data are summarized in the upcoming table and compared to average values for ambient air. Thereby, the average values of the three considered cases were used to find the minimum and maximum average value. It should be mentioned that the maximum values were measured directly after the furnace for all regarded emissions. Measurement date:

- **2010-12-09:** For this measured data, furnace 5 ran alone and was fired by a oxy/fuel

burner. The data were measured directly after the furnace

Stena Aluminum emission measurement data and a comparison with ambient air

Species	**STENA** Min.	**STENA** Max	**Air** Min.	**Air** Max.	**Unit**
CO_2	0.93	1.41	0.033	0.04	%
H_2O	2.66	3.65	1.0E−5	5	%
CO	11.16	825.85	20	25	ppm
SO_2	12.66	56.66	0.02	10	ppm
NO_2	0.50	5.85	0.1	2	ppm
N_2O	0.99	3.33	0.3	0.5	ppm
NH_3	5.80	46.94	0.3	1	ppm

Model evaluation

Six different measurement cases have been chosen to assess a representative reference case for Stena Aluminum's current process to compare the combustion of pure propane with the co-combustion of propane together with several alternatives fuel. The six cases have been chosen to cover different possible process conditions to a large extent. The oxidizer profiles are shown in figure "Oxygen profiles", whereas temperature profiles used in the different reference cases are shown in figure "Temperature profiles for different reference cases". It should be mentioned, that the secondary dilution air entering through the flute is also included in all cases. The amount of secondary air dilution is adjusted to reach the approximately an equal CO_2 concentration of 1.4 %, as it was measured by Stena Aluminum in their process directly after the furnace (date 2010-12-09) when the temperature reached 350 °C. The secondary dilution air is not changed in any of the measurement cases, since it only has dilutional effects on the process. For all measurement cases the oxygen/fuel burner is chosen to run at 2 MW, since data for oven 5, charge 604917/ 604918 from the 09-12-2010 have been provided from Stena Aluminum. At the time 11:55 in the load protocol, the burner runs at 2 - 2.5 MW and is fired by 320 Nm^3/h of oxygen introduced through the oxygen lance, which corresponds to approximately 118 g/s (λ_{O_2} = 0.752). Measurement data for the oxygen flow directly into the burner, have not been available and may be considered in a later work. The uncertainties are covered with a sensitivity analysis. The main combustion data for all cases are summarized in table "Combustion conditions of measurement cases". To adjust a diameter profile, which can be used throughout different modeling cases, a reference cumulative volumetric gas flow has been chosen, which is based on a substoichiometric oxy/fuel combustion of propane and a later injection of the theoretically sufficient amount of air for a full oxidation.

Case 1: The oxygen profile is based on data provided by Stena Aluminum (320 Nm^3/h) and considers substoichiometric conditions (λ_{O_2} = 0.752). For a dilution air profile, the amount of air theoretically necessary for a complete combustion ($\lambda_{14'000mm}$ = 1.0) is introduced after the flue gases leaving the furnace at 12'000 mm (primary dilution air). At 14'000 mm, secondary dilution air is is introduced (λ_{Total}[1] = 7.6 at 15'000 mm). Also 5 % of the primary dilution air is introduced as an air leakage into the furnace ($\lambda_{Furnace}$[2] = 0.764). The temperature profile is set at a lower peak and a lower average temperature of T_{Peak} = 2000 °C and $T_{Average}$ = 800 °C respectively.

Case 2: The oxidizer profile is not changed regarding case 1, where four times more primary dilution air is introduced as the flue gases leaving the furnace. With the increased cumulative air, also its 5 % share leaking into the UTRF increases ($\lambda_{Furnace}$ = 0.801 inside furnace). The secondary dilution air is kept constant, λ_{Total} = 7.6. The temperature profile uses T_{Peak} = 2000 °C and $T_{Average}$ = 800 °C.

Case 3: In this case the pure oxygen profile is set to a stoichiometric factor of λ_{O_2} = 1.0 to consider a stoichiometric oxy/fuel ratio, since the oxy/fuel-burner manufactured by AGA Gas AB is designed for λ_{O_2} = 1.0 at full power (4 MW). The air profile from case 1 increases $\lambda_{Furnace}$ to 1.012. With secondary dilution air lambda increases up to λ_{Total} = 7.85 at 15'000 mm. The temperature profile uses T_{Peak} = 2000 °C and $T_{Average}$ = 800 °C.

Case 4: This case uses the oxygen profile λ_{O_2} = 1.0 (case 3) as well as four times more primary dilution air (case 2), which increases $\lambda_{Furnace}$ to 1.050. With secondary dilution air λ_{Total} is increased to 7.85 at 15'000 mm. The temperature profile uses T_{Peak} = 2000 °C and $T_{Average}$ = 800 °C.

Case 5: The substoichiometric oxygen profile with λ_{O_2} = 0.752 is used. The leakage air into the furnace increases $\lambda_{Furnace}$ to 0.764. At 14'000 mm, primary dilution air increases $\lambda_{14'000mm}$ to 1.0. At 15'000 mm, λ_{Total} reaches 7.60. In this case temperature conditions are changed to higher peak and base temperatures, to consider the effect of temperature in the process. The temperature profile uses T_{Peak} = 2500 °C and $T_{Average}$ = 950 °C.

Case 6: The substoichiometric oxygen profile with λ_{O_2} = 0.752 is used to consider reducing conditions in the process. The leakage air into the furnace in increases as for this the effect on NO_x formation should be considered. Thereby $\lambda_{Furnace}$ increases to 0.9 and reaches λ_{Total} = 7.6 at 15'000 mm. The temperature profile uses T_{Peak} = 2500 °C and $T_{Average}$ = 950 °C.

[1] λ_{Total}: Total air-fuel equivalence ratio at 15'000 mm where dilution reaches its maximum.
[2] $\lambda_{Furnace}$: Air-fuel equivalence ratio inside the furnace up to 12'000 mm ($\lambda_{Furnace} = \lambda_{O_2} + \lambda_{Leakage\ air}$)

Combustion conditions of measurement cases

		Case 1	**Case 2**	**Case 3**	**Case 4**	**Case 5**	**Case 6**
P_{Burner}	[MW]	2	2	2	2	2	2
λ_{O_2} [a]	[-]	0.752	0.752	1.0	1.0	0.752	0.752
$\lambda_{\text{Leakage air}}$ [b]	[-]	0.012	0.050	0.012	0.050	0.012	0.149
λ_{Furnace} [c]	[-]	0.764	0.801	1.012	1.050	0.764	0.901
λ_{Total} [d]	[-]	7.60	7.60	7.85	7.85	7.60	7.60
T_{Average} [e]	[°C]	800	800	800	800	950	950
T_{Peak} [f]	[°C]	2000	2000	2000	2000	2500	2500

[a] λ_{O_2}: Air-fuel equivalence ratio only regarding pure oxygen.
[b] $\lambda_{\text{Leakage air}}$: Air-fuel equivalence ratio only regarding leakage air into furnace.
[c] Air-fuel equivalence ratio inside the furnace up to 12'000 mm ($\lambda_{\text{Furnace}} = \lambda_{O_2} + \lambda_{\text{Leakage air}}$).
[d] λ_{Total}: Total air-fuel equivalence ratio at 15'000 mm where dilution reaches its maximum.
[e] Average temperature inside furnace.
[f] Peak combustion temperature.

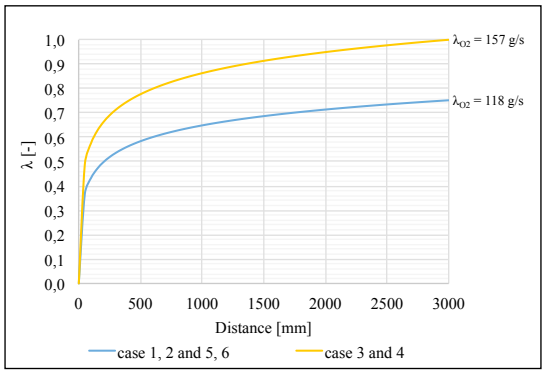

Oxygen profiles

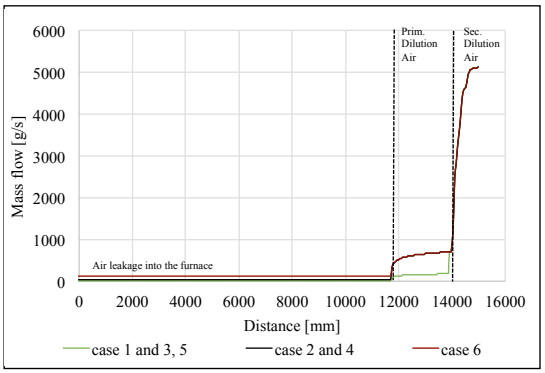

Air profiles

Oxidizer profiles for different reference cases

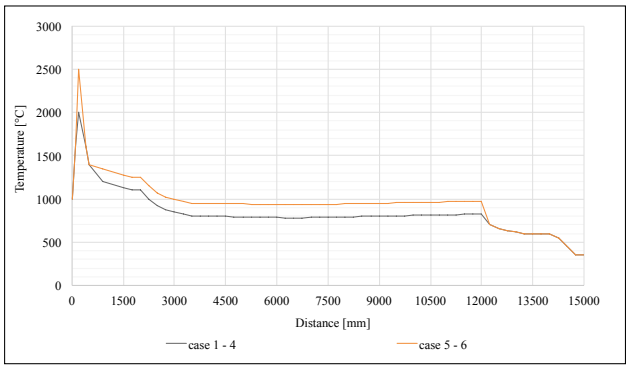

Temperature profiles for different reference cases

Selection of a reference case:

In the following section, the main results of the measurement case simulations are discussed. Thus, it is possible to show trends and effects of different process parameters on the combustion chemistry and to select a representative reference case for later co-firing simulations.
Figure "CO, CO_2 concentration for different measurement cases" shows the CO concentration and CO_2 for the six different measurement cases. The results show a complete combustion for case 3 and 4, where a small oxygen surplus is present inside the furnace (λ_{Furnace} = 1.01 and = 1.05). A higher air availability in case 4 (λ_{Furnace} = 1.05) promotes the fastest completion of combustion. The other cases show, depending on the local air availability inside the furnace, different CO concentrations for each case, which represents an incomplete combustion. After the flue gases leaving the furnace, the CO concentration decreases rapidly down to zero caused by dilution effects. The highest CO_2 concentration can be reached for case 3 and 4, where stoichiometric oxygen conditions cause a rapid completion of combustion. All other cases reach almost the same concentration inside this furnace, whereas the primary dilution after the furnace is clearly depending on the amount of introduced air. The secondary dilution causes a rapid decrease of the CO_2 concentration down to around 1.5 % for all cases, which corresponds with the measurement data provided by Stena Aluminum.

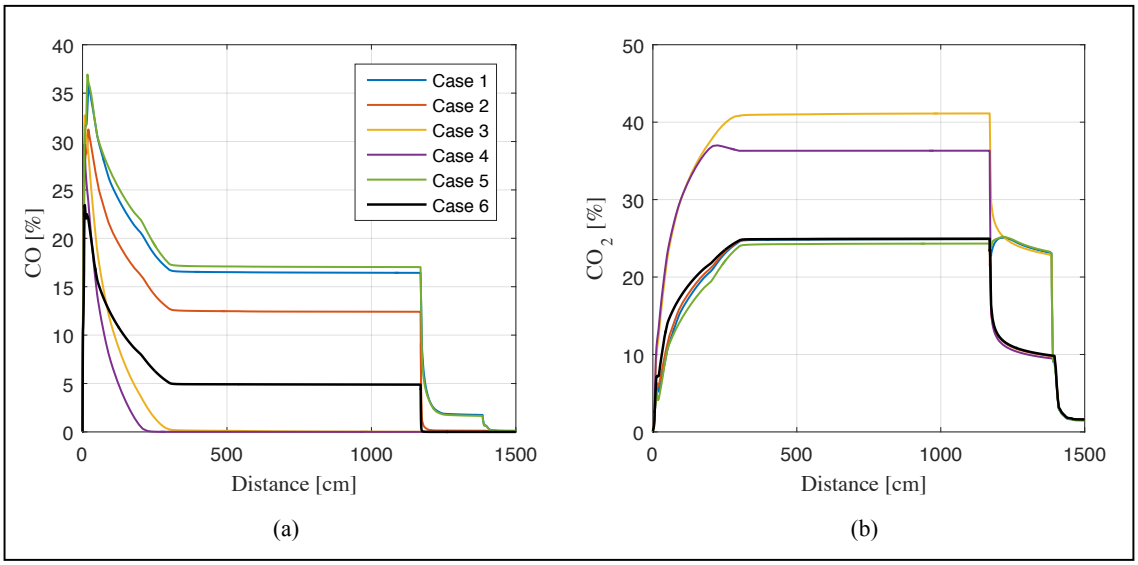

CO, CO_2 concentration for different measurement cases

Case 1: λ_{Furnace} = 0.76; λ_{Total} = 7.6; T_{Average} = 800 °C; T_{Peak} = 2000 °C / **Case 2**: λ_{Furnace} = 0.80; λ_{Total} = 7.6; T_{Average} = 800 °C; T_{Peak} = 2000 °C / **Case 3**: λ_{Furnace} = 1.01; λ_{Total} = 7.85; T_{Average} = 800 °C; T_{Peak} = 2000 °C / **Case 4**: λ_{Furnace} = 1.05; λ_{Total} = 7.85; T_{Average} = 800 °C; T_{Peak} = 2000 °C / **Case 5**: λ_{Furnace} = 0.76; λ_{Total} = 7.6; T_{Average} = 950 °C; T_{Peak} = 2500 °C / **Case 6**: λ_{Furnace} = 0.90; λ_{Total} = 7.6; T_{Average} = 950 °C; T_{Peak} = 2500 °C /

Figure "O_2, NO concentration for different measurement cases" shows the O_2 concentration for the different measurement cases. Thereby it is clearly visible that case 3 and 4 operate with an oxygen surplus coming from the additional available air inside the furnace, since O_2 concentrations of around 1 % and 3.5 % have been simulated inside the furnace, which corresponds well to the theoretically calculated λ_{Furnace} for the respective case. The NO profile shows a clear dependence on the amount of air available inside the furnace, where the combustion takes place. Also a pure temperature dependence can be seen between case 5 and the other cases. Thus, at higher peak temperatures as well as higher average temperatures inside the furnace lead to a drastic increase of the NO concentration. An increase of oxygen in case 3 showed a slight decrease of the NO concentration, whereas an increase of available air inside the furnace responded with an increase of NO emissions. In general the increase has shown the most considerable effect when both, temperature and air availability has been increased (case 6), which corresponds with the measured behavior if Stena Aluminum's facility.

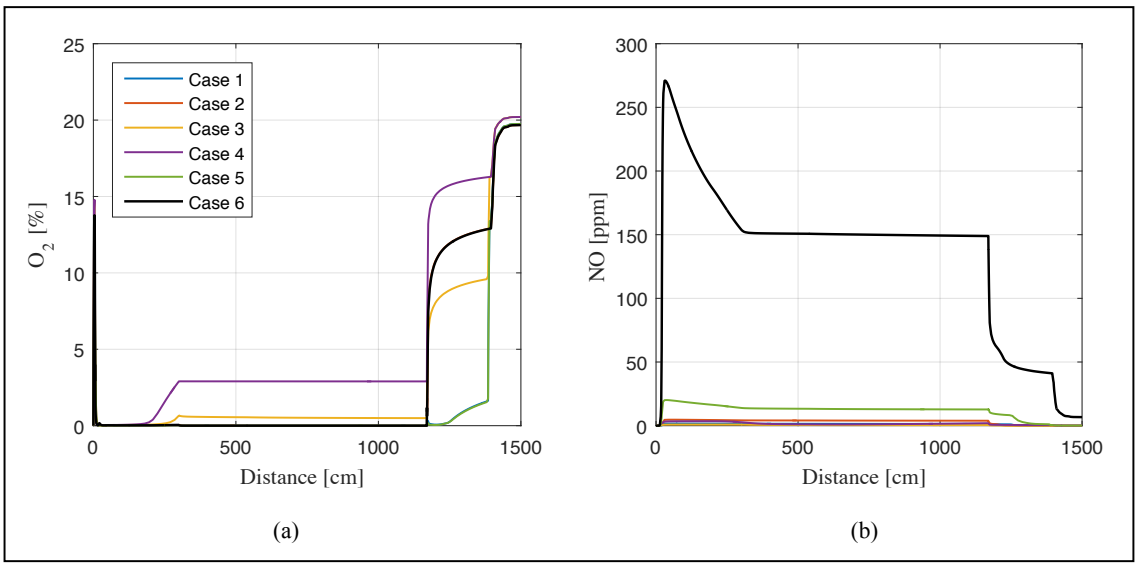

O_2, NO concentration for different measurement cases

Case 1: $\lambda_{\text{Furnace}} = 0.76$; $\lambda_{\text{Total}} = 7.6$; $T_{\text{Average}} = 800\,^{\circ}\text{C}$; $T_{\text{Peak}} = 2000\,^{\circ}\text{C}$ / **Case 2**: $\lambda_{\text{Furnace}} = 0.80$; $\lambda_{\text{Total}} = 7.6$; $T_{\text{Average}} = 800\,^{\circ}\text{C}$; $T_{\text{Peak}} = 2000\,^{\circ}\text{C}$ / **Case 3**: $\lambda_{\text{Furnace}} = 1.01$; $\lambda_{\text{Total}} = 7.85$; $T_{\text{Average}} = 800\,^{\circ}\text{C}$; $T_{\text{Peak}} = 2000\,^{\circ}\text{C}$ / **Case 4**: $\lambda_{\text{Furnace}} = 1.05$; $\lambda_{\text{Total}} = 7.85$; $T_{\text{Average}} = 800\,^{\circ}\text{C}$; $T_{\text{Peak}} = 2000\,^{\circ}\text{C}$ / **Case 5**: $\lambda_{\text{Furnace}} = 0.76$; $\lambda_{\text{Total}} = 7.6$; $T_{\text{Average}} = 950\,^{\circ}\text{C}$; $T_{\text{Peak}} = 2500\,^{\circ}\text{C}$ / **Case 6**: $\lambda_{\text{Furnace}} = 0.90$; $\lambda_{\text{Total}} = 7.6$; $T_{\text{Average}} = 950\,^{\circ}\text{C}$; $T_{\text{Peak}} = 2500\,^{\circ}\text{C}$ /

For the alternative fuel calculations, one measurement case is chosen to be considered for a later following analysis of co-combustion opportunities with alternative fuels. Thereby **case 6** has been evaluated as it considers higher temperature conditions inside the furnace as well as well a corresponding NO_x behavior. Thereby, the average temperate has been chosen to be 950 °C inside the furnace, which is a higher average temperature compared to CFD simulations by B. Zhou et al. [94] but lower compared to the considered average temperature of 1100 °C chosen in Stena Metall's report "Calculation of gas flow and pressure drop around the rotary kiln furnace Älmhult" from the 2011-05-13 by Björn Hall. However, the average temperature conditions inside the furnace could be covered in a later sensitivity analysis. The outgoing CO_2 concentration (at 15'000 mm) is almost equal for all alternatives, since primary and secondary dilution air cause a rapid decrease of the CO_2 down to around 1.5 %, which corresponds with the maximum measurement data provided by Stena Aluminum (table **??**) and measured directly after the furnace. Thus, the dilutional effects considered in the simulations can be assumed to represent Stena Aluminum's process to a valuable extent. Additionally, case 6 considers a higher air availability inside the furnace but substoichiometric conditions regarding pure oxygen feeding, which corresponds well with Stena Aluminum's process conditions. Since no measurement data for air leakage and temperature conditions inside the furnace have been available, it should be remarked that the simulations can only show trends and an overall behavior but will not represent the real process. Furthermore, the overall stoichiometry inside the furnace is kept constant at $\lambda_{\text{Furnace}} = 0.9$ for all co-firing simulations. Therefore, the oxygen profiles had to be adapted for each fuel alternative, since different oxygen requirements per MJ lead to differing behaviors compared to a pure propane combustion. For all fuel alternatives, the co-firing simulations were made regarding a power of 2 MW for the burner, fired by **60 % of propane** and **40 % of alternative fuel** on an energy basis (regarding LHVs). For the later choice of certain fuel alternatives, which are going to be analyzed in more detail and covered in a sensitivity analysis, the yearly availability for Stena Recycling International in Sweden is an important factor, since a future change to co-firing may be highly depended on the availability and security of supply for the selected waste-derived fuel. Regarding this criteria, the focus should be based on SLF, PFO, WEEE (Incineration) and WEEE (Landfill) as theses waste-derived fuels show the highest availability, with 65'000 tons/yr, 28'000 tons/yr and both 5'000 tons/yr respectively.

Appendix D.

Appendix: Economic evaluation

Calculation of potential economic savings

	PFO	**SLF**	**WEEE$_{\text{Inc.}}$**	**Unit**
λ_{O_2}	0.75	0.75	0.75	
Req. O_2 alt. fuel	80.0	131.8	64.4	$^{g}/_{MJ}$
Req. O_2 for C_3H_8	78.8	78.8	78.8	$^{g}/_{MJ}$
Share of C_3H_8	0.6	0.6	0.6	
$P_{alt.fuel}$	2	2	2	MW
$P_{C_3H_8}$	3	3	3	MW
Load factor	0.7	0.7	0.7	
$E_{alt.fuel}$	44.2	44.2	44.2	TJ/yr
$E_{C_3H_8}$	66.2	66.2	66.2	TJ/yr
$LHV_{alt.fuel}$	41.4	14.3	30.1	MJ/kg
$LHV_{C_3H_8}$	46.1	46.1	46.1	MJ/kg
$m_{alt.fuel}$	1066	3087	1467	tons/yr
$m_{C_3H_8}$	1435	1435	1435	tons/yr
mO_2 alt.fuel	2659	4380	2308	tons/yr
m_{O_2} prop.	3931	3931	3931	tons/yr
$m_{O_2,total}$	6589	8311	6239	tons/yr
Δ_{O_2} [a]	**+0.8**	**+27.1**	**-4.6**	%
Cost of C_3H_8	1	1	1	SEK/l
Cost of alt. fuel	0.01	0.2	0.3	
$C_{C_3H_8,total}$	2.92	2.92	2.92	Mio. SEK
$C_{alt.fuel,total}$	0.01	0.62	0.44	Mio. SEK
C_{Total}	2.93	3.54	3.36	Mio. SEK
ΔC [b]	**-40**	**-27**	**-31**	%

[a] Change in O_2 consumption compared to firing with pure propane at a stoichiometry of $\lambda = 0.75$
[b] Change in fuel cost compared to firing with pure propane at 5 MW average power.